

# Auxiliary MCMC and particle Gibbs samplers for parallelisable inference in latent dynamical systems

Adrien Corenflos, Simo Särkkä

Department of Electrical Engineering and Automation, Aalto University

March 2, 2023

## Abstract

We introduce two new classes of exact Markov chain Monte Carlo (MCMC) samplers for inference in latent dynamical models. The first one, which we coin auxiliary Kalman samplers, relies on finding a linear Gaussian state-space model approximation around the running trajectory corresponding to the state of the Markov chain. The second, that we name auxiliary particle Gibbs samplers corresponds to deriving good local proposals in an auxiliary Feynman–Kac model for use in particle Gibbs. Both samplers are controlled by augmenting the target distribution with auxiliary observations, resulting in an efficient Gibbs sampling routine. We discuss the relative statistical and computational performance of the samplers introduced, and show how to parallelise the auxiliary samplers along the time dimension. We illustrate the respective benefits and drawbacks of the resulting algorithms on classical examples from the particle filtering literature.

## 1 Introduction

For a given finite horizon  $T > 0$ , state-space models (SSMs, see, e.g., [Del Moral, 2004](#); [Särkkä, 2013](#); [Chopin and Papaspiliopoulos, 2020](#)), also called hidden Markov models, are a class of models which are fully described by the joint distribution of the states and observations:

$$\mathbb{P}(dx_{0:T}, dy_{0:T}) := \mathbb{P}_0(dx_0) \left\{ \prod_{t=0}^T H_t(dy_t | x_t) \right\} \left\{ \prod_{t=1}^T P_t(dx_t | x_{t-1}) \right\}. \quad (1)$$

In this formulation,  $\mathbb{P}_0$  represents the initial distribution of the state  $X_0$ , while  $P_t$  and  $H_t$  represent the Markov transition and emission kernels for the states  $X_t \in \mathbb{R}^{d_x}$  and observations  $Y_t \in \mathbb{R}^{d_y}$ , respectively.

Inference in SSMs typically has different meanings depending on the context: filtering is concerned with representing, sampling, or computing expectations of the quantity  $\mathbb{P}(dx_t | y_{0:t})$ , where  $y_{0:t} = \{y_i; i = 0, 1, \dots, t\}$ ; marginal smoothing is concerned with the same problems for the quantity  $\mathbb{P}(dx_t | y_{0:T})$ ; and pathwise smoothing is concerned with sampling or computing expectations of the quantity  $\mathbb{P}(dx_{0:T} | y_{0:T})$ . Furthermore, in many cases, the “true” generative model, consisting of the initial distribution  $\mathbb{P}_0$ , the transition kernels  $P_t$ , and emission kernels  $H_t$ , is unknown, and one needs to estimate it from the observed data. A typical way is to assume parametric forms for  $\mathbb{P}_0(dx_0 | \theta)$ ,  $P_t(dx_t | x_{t-1}, \theta)$ , and  $H_t(dy_t | x_t, \theta)$ , as well as a prior distribution  $\mathbb{P}(d\theta)$  for the parameters, resulting in a joint distribution

$$\mathbb{P}(dx_{0:T}, dy_{0:T}, d\theta) := \mathbb{P}_0(dx_0 | \theta) \left\{ \prod_{t=0}^T H_t(dy_t | x_t, \theta) \right\} \left\{ \prod_{t=1}^T P_t(dx_t | x_{t-1}, \theta) \right\} \mathbb{P}(d\theta). \quad (2)$$

The parameter estimation problem then consists in computing either deterministic or probabilistic estimates of the posterior distribution of parameters  $\mathbb{P}(d\theta | y_{0:T})$ . In this work, we will focus on computing probabilistic estimates for the pathwise smoothing distribution  $\mathbb{P}(dx_{0:T} | y_{0:T})$ , the parameters distribution  $\mathbb{P}(d\theta | y_{0:T})$ , and the joint posterior distribution  $\mathbb{P}(d\theta, dx_{0:T} | y_{0:T})$ .

Throughout the rest of the article, we will assume that all distributions and kernels considered have a density with respect to the corresponding Lebesgue measure, and we consequently will write

$$p(x_{0:T}, y_{0:T}, \theta) := p_0(x_0 | \theta) \left\{ \prod_{t=0}^T h_t(y_t | x_t, \theta) \right\} \left\{ \prod_{t=1}^T p_t(x_t | x_{t-1}, \theta) \right\} p(\theta). \quad (3)$$

Moreover, when it is not harmful, the dependency on the parameters  $\theta$  will be made implicit, and the methods will be presented for known models.

A natural generalisation of (3) is given by the class of models

$$\pi(x_{0:T}) \propto g(x_0, x_1, \dots, x_T) p_0(x_0) \left\{ \prod_{t=1}^T p_t(x_t | x_{t-1}) \right\}, \quad (4)$$

which recover, as a special case, the pathwise smoothing formulation  $p(x_{0:T} | y_{0:T})$  of (2) with

$$g(x_0, x_1, \dots, x_T) = \prod_{t=0}^T h_t(y_t | x_t). \quad (5)$$

It also recovers the class of Feynman-Kac models (see, e.g., [Del Moral, 2004](#)) with tractable transitions

$$\pi(x_{0:T}) \propto g_0(x_0) p_0(x_0) \left\{ \prod_{t=1}^T g_t(x_t, x_{t-1}) p_t(x_t | x_{t-1}) \right\}, \quad (6)$$

by setting  $g(x_0, x_1, \dots, x_T) = g_0(x_0) \prod_{t=1}^T g_t(x_t, x_{t-1})$ . Under this more general formalism, the marginal smoothing problem corresponds to computing the quantity  $\pi(x_t)$  for a given  $t$ , while pathwise smoothing aims at the full distribution  $\pi(x_{0:T})$ .

Two popular classes of methods for inference in SSMs are the Gaussian approximation based methods (i.e., Kalman filters and smoothers), and the sequential Monte Carlo (SMC) based methods (i.e., particle filter and smoothers). These classes of methods are briefly reviewed next in Sections 1.1 and 1.2.

## 1.1 Gaussian approximated state-space models

Gaussian approximations rely on the fact that when the SSM at hand is linear Gaussian (LGSSM), then the filtering and marginal smoothing distributions are Gaussian as well, and their means and covariances can be computed sequentially and in closed form (see, e.g., [Särkkä, 2013](#); [Barfoot, 2017](#)). This is leveraged in Gaussian approximations to the filtering and marginal smoothing solutions of general SSMs. Typically, such approximations rely on Taylor linearisation, leading to the classical extended Kalman filtering (see, e.g., [Jazwinski, 1970](#)), or on sigma-point linearisations, first introduced in [Julier and Uhlmann \(2004\)](#); [Wan and Van Der Merwe \(2000\)](#). In this work we will focus on a more general posterior linearisation framework encompassing both methods and recently introduced in [García-Fernández et al. \(2017\)](#); [Tronarp et al. \(2018\)](#). See Section 2.3 for a short review of these methods in the context of this work.

The state of the art for these methods consists in iteratively reusing the approximated marginal smoothing distributions to refine the Gaussian approximation of the SSM at hand ([Bell, 1994](#); [García-Fernández et al., 2017](#); [Tronarp et al., 2018](#)). Doing so makes it possible to handle SSMs for which the reverse Markov chain representing the smoothing distribution is a slow-mixing process, that is, SSMs which have “sticky” transitions kernels and for which the filtering transition largely differs from the smoothing one. These recursive methods have been shown to be equivalent to certain minimisation programs (such as Gauss–Newton) for some given loss functions and to be (locally) convergent. For a review of these methods we refer the reader to the doctoral thesis of [Tronarp \(2020\)](#).

Furthermore, it has been recently shown ([Särkkä and García-Fernández, 2021](#); [Yaghoobi et al., 2021, 2022](#)) that these iterative methods can be parallelised in time (PIT), resulting in a computational complexity of  $\mathcal{O}(\log(T))$  on parallel hardware such as graphics processing units (GPUs), comparing to their classical  $\mathcal{O}(T)$  complexity on sequential hardware.

An important drawback of all the Gaussian approximation based methods is that they (in all but the LGSSM case) result in biased estimates of the true filtering distribution as well as marginal and pathwise smoothing distributions. This bias is also present in the normalisation constant estimate (marginal likelihood of the observations) of the model, which makes the parameter estimation biased as well.

## 1.2 Sequential Monte Carlo

Sequential Monte Carlo (SMC) methods (see, e.g., [Chopin and Papaspiliopoulos, 2020](#)) are based on approximating the filtering and smoothing distributions using Monte Carlo samples drawn from these distributions. They then propagate the trajectory by sequentially applying a sampling-resampling routine. Notably, SMC methods (aside from the family of marginal particle filtering methods, see, [Klaas et al.,](#)

2005) provide a representation of the full pathwise smoothing distribution. This representation converges when the number of samples tends to infinity (Kitagawa, 1996). However, in practice, the resulting paths are degenerate for time steps  $t \ll T$ . This has justified the introduction of backward weighting and sampling methods to rejuvenate the trajectories far from the endpoint (Godsill et al., 2004a), and their resulting convergence improvements have been studied, for example in Douc et al. (2011), and more recently under a more general framework, in Dau and Chopin (2022).

Because particle filtering methods provide an unbiased likelihood estimate, they can be used to perform parameter estimation in state-space models. A particularly useful class of methods leveraging this property are the particle Markov chain Monte Carlo (pMCMC) methods (Andrieu and Roberts, 2009; Andrieu et al., 2010), which are based on constructing MCMC schemes either as a Metropolis–Rosenbluth–Teller–Hastings (MRTH) algorithm (Metropolis et al., 1953; Hastings, 1970), or a Gibbs-like sampler (Geman and Geman, 1984). We will refer to these two classes of algorithms as pseudo-marginal and particle Gibbs (pGibbs), respectively. The asymptotic properties of pGibbs schemes in particular have been the subject of many investigations, and increasingly stronger convergence results have been successfully derived for them, for example, in Chopin and Singh (2015); Andrieu et al. (2018); Lee et al. (2020).

These two methods sample consistently from the (joint) pathwise smoothing and parameter posterior distributions in general SSMs, but numerically fail when the transition kernel is “sticky”, or when the latent space dimension is large. Ancestor sampling methods (Whiteley, 2010; Lindsten et al., 2014) can be, to some extent, used to mitigate this problem. However, the failure is due to the inherent property that the set of particles available to describe the smoothing distribution comes from the forward filtering pass in the first place. Thus, the weights appearing during the backward pass of either the smoothing or particle Gibbs algorithm will exhibit a large variance. Recently, Finke and Thiery (2023) and Malory (2021, Chap. 4) independently proposed related particle Gibbs algorithms that alleviate this issue. Finke and Thiery (2023) in particular showed that under a proper scaling of their algorithms, the methods do not suffer from the curse of dimensionality present in classical particle MCMC methods. In this article, we consider the formulation of Finke and Thiery (2023).

Finally, it was recently shown in Corenflos et al. (2022) that divide-and-conquer methods can be leveraged to provide consistent PIT solutions for smoothing, pMCMC and pGibbs algorithms at the cost of additional variance in the resulting estimates, providing a SMC counterpart to the algorithms of Särkkä and García-Fernández (2021); Yaghoobi et al. (2021, 2022).

### 1.3 Outline and Contributions

As a summary of the sections above, the Gaussian approximated smoothing solutions, whilst being more robust than SMC methods (and extensions thereof), lack the unbiasedness and convergence properties of these. This motivates the following contributions of this article:

1. In Section 2, we show that, in the case of generalised Feynman–Kac models (4) with Gaussian dynamics, the auxiliary proposals of Titsias and Papaspiliopoulos (2018) recover the posterior distribution of an auxiliary LGSSM. We leverage this to reduce their time and space complexity to  $\mathcal{O}(T)$  rather than  $\mathcal{O}(T^3)$ . We then use the generalised statistical regression framework of Tronarp et al. (2018) to derive a new class of LGSSM auxiliary samplers for non-Gaussian latent dynamical systems.
2. In Section 3, we introduce two parallel-in-time samplers for LGSSM pathwise smoothing distributions, one based on a prefix-sum implementation akin to Särkkä and García-Fernández (2021), and the other based on a divide-and-conquer recursion. We use these to sample from the LGSSM proposals, resulting in an overall  $\mathcal{O}(\log T)$  MCMC algorithm on parallel hardware.
3. In Section 4, we extend the construction of Section 2 to the context of particle MCMC. This will allow us to tackle models for which Gaussian approximations are not practical or under-performing. We show that Finke and Thiery (2023) is recovered as a special case of our method.
4. In Section 5, we illustrate the proposed methods on a series of examples from the SMC and Gaussian approximated inference literature. Special attention is paid to understanding their statistical as well as time and memory trade-offs.

## 2 Auxiliary Kalman samplers

In this section, we first review the auxiliary gradient-based samplers of [Titsias and Papaspiliopoulos \(2018\)](#), and then show that when the latent model consists of Gaussian dynamics, they can be reformulated in terms of the posterior distribution of an auxiliary LGSSM. This reduces their computational complexity to linear, as opposed to cubic, in the number of time steps. This perspective will serve as a building block for the rest of the methods presented in this article.

### 2.1 Auxiliary gradient-based samplers

Auxiliary gradient-based methods were introduced in [Titsias and Papaspiliopoulos \(2018\)](#) as a way to construct posterior-informed proposals in MCMC samplers for Gaussian latent models with a density  $\pi(x) \propto \exp(f(x))\mathcal{N}(x; 0, C)$ <sup>1</sup>, where  $x \in \mathbb{R}^{d_x}$ . They were shown to outperform classical preconditioned (prior-informed) and gradient-based (likelihood-informed) samplers for latent Gaussian models.

Auxiliary gradient-based samplers rely on augmenting the target  $\pi$  with an auxiliary variable  $u$ :

$$\pi(x, u) \propto \exp(f(x))\mathcal{N}(x; 0, C)\mathcal{N}\left(u; x, \frac{\delta}{2}I\right), \quad (7)$$

where  $\delta > 0$  is a step size, so that the marginal of  $\pi(x, u)$  is  $\pi(x)$ . Auxiliary samplers then proceed by linearising  $f$  around the current state  $x$  of the Markov chain to obtain a Gaussian proposal distribution

$$\begin{aligned} q(y | x, u) &\propto \exp(\nabla f(x)^\top y)\mathcal{N}(y; 0, C)\mathcal{N}\left(u; y, \frac{\delta}{2}I\right) \\ &= \mathcal{N}\left(y; \frac{2}{\delta}A\left(u + \frac{\delta}{2}\nabla f(x)\right), A\right), \end{aligned} \quad (8)$$

where  $A = \frac{\delta}{2}(C + \frac{\delta}{2}I)^{-1}C = (C^{-1} + \frac{2}{\delta}I)^{-1}$ . Sampling from  $\pi(x, u)$  (and therefore from  $\pi(x)$  by discarding the intermediate auxiliary steps) is then done via Hastings-within-Gibbs ([Müller, 1993](#)):

1. Sample  $u | x \sim \mathcal{N}(u; x, \frac{\delta}{2}I)$ .
2. Propose  $y \sim q(\cdot | x, u)$  targeting  $\pi(\cdot | u) \propto \pi(\cdot, u)$ , and accept the move with the corresponding acceptance probability.

A more efficient counterpart of this, targeting  $\pi(x)$  directly, can be given by integrating the proposal distribution (8) with respect to  $\mathcal{N}(u; x, \frac{\delta}{2}I)$ :

$$q(y | x) = \mathcal{N}\left(y; \frac{2}{\delta}A\left(x + \frac{\delta}{2}\nabla f(x)\right), \frac{2}{\delta}A^2 + A\right). \quad (9)$$

This marginalised version skips the intermediate sampling step of the auxiliary variable, and is provably better – both empirically and in terms of Peskun ordering ([Peskun, 1973](#); [Tierney, 1998](#); [Leisen and Mira, 2008](#)) – than its auxiliary version, resulting in step sizes  $\delta$  roughly twice larger (see Tables 1, 2, and 3 in [Titsias and Papaspiliopoulos, 2018](#)) for the same acceptance rate, at virtually no additional computational complexity.

A crucial property of both these instances of the auxiliary sampler is that for all  $\delta > 0$ , the matrices  $A$  and  $C$  share the same eigenspace ([Titsias and Papaspiliopoulos, 2018](#), Section 3.3). This ensures that after an initial spectral decomposition of  $C$ , changing the value of  $\delta$  can be done at a negligible cost compared to the actual sampling process itself, making the algorithm easy to tune for a given target acceptance rate.

However, when  $C$  depends on a parameter  $\theta$ , changing  $\theta$  will not keep the eigenspace invariant. This means that when using either of these samplers within a Hastings-within-Gibbs routine targeting a joint model  $\pi(x, \theta) \propto \exp(f(x))\mathcal{N}(x; 0, C_\theta)p(\theta)$ , the spectral decomposition of  $C_\theta$  has to be recomputed every time the value of  $\theta$  changes. This is computationally prohibitive for large dimensional  $x$ . This, however, can be mitigated thanks to the following observation ([Titsias and Papaspiliopoulos, 2018](#)): under a reparametrisation of  $u$ , which corresponds to considering the augmented target

$$\pi(x, u) \propto \exp(f(x))\mathcal{N}(x; 0, C)\mathcal{N}\left(u; x + \frac{\delta}{2}\nabla f(x), \frac{\delta}{2}I\right), \quad (10)$$

---

<sup>1</sup>As well as, under a trivial change of variables, for models with non-zero prior mean.

rather than (7), the proposal distribution  $q(y | x, u)$  can be made independent of the current state of the chain  $x$ . This allows doing joint updates of  $x$  and  $\theta$  in parametric models, rather than using Gibbs steps to sample  $x$  conditionally on  $\theta$ , and  $\theta$  conditionally on  $x$ , thereby improving the mixing rate of the sampled Markov chain. This improvement, however, does not change the need for updating the spectral decomposition of  $C_\theta$  and comes at the price of a lower statistical efficiency than the non-reparametrised version.

## 2.2 Auxiliary Kalman samplers

The proposal (8) covers latent Gaussian models in general, and in particular covers models with latent Gaussian dynamics<sup>2</sup>:

$$\begin{aligned} \pi(x_{0:T}) &\propto g(x_0, \dots, x_T) \\ &\times \mathcal{N}(x_0; m_0, P_0) \prod_{t=1}^T \mathcal{N}(x_t; F_{t-1} x_{t-1} + b_{t-1}, Q_{t-1}). \end{aligned} \quad (11)$$

However, directly treating these as latent Gaussian models would incur a computational complexity of  $\mathcal{O}(T^2 d_x^2)$ , with an initial pre-processing step that scales as  $\mathcal{O}(T^3 d_x^3)$ , and a memory cost of  $\mathcal{O}(T^2 d_x^2)$  corresponding to the size of the underlying covariance matrix  $C$ . This is true even though the inverse of  $C$  is sparse (see, e.g., Barfoot, 2017, Chap. 3) due to the need to compute the eigen-decomposition of either  $C$  or  $C^{-1}$  (Titsias and Papaspiliopoulos, 2018, Supplementary material). Instead of doing this, it is possible, in the case of a model like (11), to preserve the Markovian structure of the model and formulate the auxiliary sampler as a LGSSM, which can then be used more efficiently.

In order to do so, we emulate Titsias and Papaspiliopoulos (2018), and consider the augmented target distribution

$$\pi(x_{0:T}, u_{0:T}) \propto \pi(x_{0:T}) \prod_{t=0}^T \mathcal{N}\left(u_t; x_t, \frac{\delta}{2} \Sigma_t\right), \quad (12)$$

where  $\delta > 0$  and, for all  $t = 0, \dots, T$ ,  $\Sigma_t$  is some positive definite matrix in  $\mathbb{R}^{d_x \times d_x}$ . Note that when  $\Sigma_t = I$  is the identity matrix for all  $t$ , this recovers the proposal (7).

Let us define  $\gamma$  via  $\exp(\gamma(x_0, x_1, \dots, x_T)) := g(x_0, x_1, \dots, x_T)$ , and linearise it around the previously sampled trajectory  $x_{0:T}$ ,

$$\gamma(z_{0:T}) \approx \gamma(x_{0:T}) + \langle v_{0:T}, z_{0:T} - x_{0:T} \rangle, \quad (13)$$

where  $v_t = \frac{\partial \gamma}{\partial x_t}(x_{0:T})$  for all  $t$ , and  $\langle a_{0:T}, b_{0:T} \rangle$  denotes the sum of inner products  $\sum_{t=0}^T \langle a_t, b_t \rangle$ .

Under these notations, we can define the auxiliary proposal

$$\begin{aligned} q(z_{0:T} | u_{0:T}, x_{0:T}) &\propto \mathcal{N}(z_0; m_0, P_0) \left\{ \prod_{t=1}^T \mathcal{N}(z_t; F_{t-1} z_{t-1} + b_{t-1}, Q_{t-1}) \right\} \\ &\left\{ \prod_{t=0}^T \mathcal{N}\left(u_t + \frac{\delta}{2} \Sigma_t v_t; z_t, \frac{\delta}{2} \Sigma_t\right) \right\}, \end{aligned} \quad (14)$$

which corresponds to the pathwise smoothing distribution of a LGSSM with unchanged dynamics compared to (11), and observations given by  $u_t + \frac{\delta}{2} \Sigma_t v_t$  for an observation model  $\mathcal{N}(\cdot; z_t, \frac{\delta}{2} \Sigma_t)$ ,  $t = 0, 1, \dots, T$ . Sampling from this distribution, and evaluating its likelihood can be done using Kalman primitives (see, e.g. Särkkä, 2013, Ch. 4 and Ch. 8) in  $\mathcal{O}(T)$  steps. In fact, this representation is crucial to reduce the memory requirements to linear in  $T$  as well as the computational complexity from cubic to linear or even logarithmic in  $T$  for parallel hardware. We come back to this last point in Section 3.

We insist that this proposal is statistically equivalent to the auxiliary method of Titsias and Papaspiliopoulos (2018) for a choice of constant  $\Sigma_t = I$ , but exhibits better computational complexity. Marginalising it, however, would destroy the latent Markovian structure, removing this advantage completely. Similarly, in general, a second order approximations of  $\gamma$  would result in fully dependent observations, so that the proposal distribution would not correspond to a LGSSM anymore. An important

---

<sup>2</sup>This was in fact explicitly used in Chopin and Papaspiliopoulos (2020, Chap. 15), where the authors successfully apply the marginal sampler (9) to a one-dimensional stochastic volatility model with latent Gaussian dynamics. The fact that the auxiliary sampler corresponded to a LGSSM was, however, not noted by the authors.

special case, however, is that of separable potentials, as is the case for state-space models. Indeed, when  $g(x_{0:T}) = \prod_{t=0}^T g_t(x_t)$ , or equivalently, when  $\gamma(x_{0:T}) = \sum_{t=0}^T \gamma_t(x_t)$ , we can write

$$\gamma(z_{0:T}) \approx \gamma(x_{0:T}) + \langle v_{0:T}, z_{0:T} - x_{0:T} \rangle + \frac{1}{2} \sum_{t=0}^T (z_t - x_t)^\top \Lambda_t (z_t - x_t), \quad (15)$$

where  $\Lambda_t$  is the Hessian matrix of  $\gamma_t$  evaluated at  $x_t$ . By rearranging the terms, we can derive the resulting proposal distribution as

$$q(z_{0:T} \mid u_{0:T}, x_{0:T}) \propto \mathcal{N}(z_0; m_0, P_0) \left\{ \prod_{t=1}^T \mathcal{N}(z_t; F_{t-1}z_{t-1} + b_{t-1}, Q_{t-1}) \right\} \left\{ \prod_{t=0}^T \mathcal{N}(\omega_t; z_t, \Omega_t) \right\}, \quad (16)$$

with

$$\Omega_t = \left( \frac{2}{\delta} \Sigma_t^{-1} - \Lambda_t \right)^{-1} \quad \text{and} \quad \omega_t = \Omega_t \left( \frac{2}{\delta} \Sigma_t^{-1} u_t + v_t - \Lambda_t x_t \right). \quad (17)$$

This proposal is well defined as a LGSSM as soon as  $\delta$  is small enough. We note that other choices for  $\Lambda_t$  are possible (for example using low-rank approximations of the Hessian matrix), and that this formula can be used as an approximation of a second-order decomposition when the potentials are not separable. These would however be *ad-hoc* methods, and we do not discuss them further in this article.

Finally, when the dynamics are not Gaussian, it is often possible to transform the model at hand into an equivalent representation of  $q_{0:T}$  with Gaussian dynamics by setting

$$\begin{aligned} p_0(x_0) &\leftarrow \mathcal{N}(x_0; m_0, P_0) \\ p_t(x_t \mid x_{t-1}) &\leftarrow \mathcal{N}(x_t; F_{t-1}x_{t-1} + b_{t-1}, Q_{t-1}) \\ g(x_{0:T}) &\leftarrow g(x_{0:T}) \frac{p_0(x_0)}{\mathcal{N}(x_0; m_0, P_0)} \prod_{t=1}^T \frac{p_t(x_t \mid x_{t-1})}{\mathcal{N}(x_t; F_{t-1}x_{t-1} + b_{t-1}, Q_{t-1})}. \end{aligned} \quad (18)$$

This family of techniques is at the core of guided and auxiliary particle filtering methods (see, e.g., [Chopin and Papaspiliopoulos, 2020](#), Ch. 10). While this is sometimes a natural thing to do, for example when the transition kernel is the product of a linear Gaussian transition and another term, it can also happen that there is no natural way to make such a Gaussian appear in the model. This justifies the need for introducing a new class of auxiliary samplers.

### 2.3 New auxiliary samplers for models with tractable conditional moments

In Section 2.2, we have made an explicit link between the auxiliary samplers of [Titsias and Papaspiliopoulos \(2018\)](#) and Kalman filtering when the latent model has Gaussian dynamics. This linearity of the latent model corresponds to the assumption of linear Gaussian dynamics in the case of state-space models. This is a rather strong modeling assumption that is not easily verified, or enforced, in practice. In this section, we present an approach which uses local approximations of the dynamics model by conditional Gaussians using statistical linear regression.

In order to present the method in its most general form, we consider the case of state-space models, where the potential function  $g(x_{0:T})$  corresponds to a product of observation models  $\prod_{t=0}^T h_t(y_t \mid x_t)$  so that we can also form the Gaussian approximation to the potential itself. Following [Tronarp et al. \(2018\)](#), we suppose that the first two conditional moments

$$\begin{aligned} m^X(x_{t-1}) &:= \mathbb{E}[X_t \mid X_{t-1} = x_{t-1}], & m^Y(x_t) &:= \mathbb{E}[Y_t \mid X_t = x_t], \\ V^X(x_{t-1}) &:= \mathbb{V}[X_t \mid X_{t-1} = x_{t-1}], & V^Y(x_t) &:= \mathbb{V}[Y_t \mid X_t = x_t], \end{aligned} \quad (19)$$

of, respectively, the transitions and observation models appearing in (1) can easily be either computed in closed form, or approximated well enough. Similarly, we suppose that the two first moments  $m_0$  and  $P_0$  of  $p_0$  are known at least approximately.

Similarly as in Section 2.2, we start by considering an augmented target distribution

$$p(x_{0:T}, y_{0:T}, u_{0:T}) := p(x_0) \left\{ \prod_{t=0}^T h_t(y_t \mid x_t) \mathcal{N}(u_t; x_t, \frac{\delta}{2} \Sigma_t) \right\} \left\{ \prod_{t=1}^T p_t(x_t \mid x_{t-1}) \right\}, \quad (20)$$

where  $\delta > 0$ , and for all  $t$ ,  $\Sigma_t$  is a positive definite matrix.

In order to form a proposal distribution  $q(x_{0:T} | u_{0:T}, y_{0:T})$  for  $p(x_{0:T} | y_{0:T}, u_{0:T})$ , we linearise the state-space model (1) around the trajectory at hand. Let  $x_{0:T} \in \mathbb{R}^{T \times d_x}$  and  $u_{0:T} \in \mathbb{R}^{T \times d_x}$  be the current states of the auxiliary Markov chain, and let  $\Gamma_{0:T}$  be a set of reference covariance matrices in  $\mathbb{R}^{T \times d_x \times d_x}$ , by which we mean that  $\Gamma_t \in \mathbb{R}^{d_x \times d_x}$  needs to be positive definite for all  $t$ . We can apply the generalised statistical linear regression (GSLR) framework of [Tronarp et al. \(2018\)](#) for the reference random variables  $\zeta_t \sim \mathcal{N}(x_t, \Gamma_t)$ ,  $t = 0, \dots, T$  to derive Gaussian approximations of the transition and observation models as follows:

$$\begin{aligned} p_t(z_t | z_{t-1}) &\approx \mathcal{N}(z_t; F_{t-1}z_{t-1} + b_{t-1}, Q_{t-1}), \\ h_t(y_t | z_t) &\approx \mathcal{N}(y_t; H_t z_t + c_t, R_t), \end{aligned} \quad (21)$$

with,

$$\begin{aligned} F_{t-1} &= C_{t-1}^X \Gamma_{t-1}^{-1}, & H_t &= C_t^Y \Gamma_t^{-1}, \\ b_{t-1} &= \mu_{t-1}^X - F_{t-1} x_{t-1}, & c_t &= \mu_t^Y - H_t x_t, \\ Q_{t-1} &= S_{t-1}^X - F_{t-1} \Gamma_{t-1}^{-1} F_{t-1}^\top, & R_t &= S_t^Y - H_t \Gamma_t^{-1} H_t^\top, \end{aligned} \quad (22)$$

and where, for the sake of readability, we do not notationally emphasise the dependency on  $x$  and  $\Gamma$ . These Gaussian approximations are known to minimise a forward KL divergence with respect to the transition and observation models for the Gaussian variational family. The coefficients appearing in (22) are in turn given by the general formulae

$$\begin{aligned} C_{t-1}^X &= \mathbb{C} [m^X(\zeta_{t-1}), \zeta_{t-1}], & C_t^Y &= \mathbb{C} [m^Y(\zeta_t), \zeta_t], \\ \mu_{t-1}^X &= \mathbb{E} [m^X(\zeta_{t-1})], & \mu_t^Y &= \mathbb{E} [m^Y(\zeta_t)], \\ S_{t-1}^X &= \mathbb{E} [V^X(\zeta_{t-1})], & S_t^Y &= \mathbb{E} [V^Y(\zeta_t)]. \end{aligned} \quad (23)$$

Clearly, the quantities in (23) are not typically available in closed-form, and we instead need to resort to further approximations. Such approximations are given by, for example, Taylor series expansions or sigma-point methods, such as Gauss–Hermite or unscented methods (see, e.g., [Särkkä, 2013](#), Ch. 5).

**Example 2.1.** *The first-order Taylor approximation to  $C_{t-1}^X$  can be obtained by  $m^X(\zeta_{t-1}) \approx m^X(x_{t-1}) + \nabla m^X(x_{t-1})(\zeta_{t-1} - x_{t-1})$ , giving  $C_{t-1}^X \approx \nabla m^X(x_{t-1}) \Gamma_{t-1}$ , and finally  $F_{t-1} \approx \nabla m^X(x_{t-1})$ . When the model at hand has additive Gaussian noise:  $X_t = f(x_{t-1}) + \epsilon_{t-1}$ , this recovers the well-known extended Kalman filter linearisation. Similarly, all the other linearisation parameters will be independent of the choice of  $\Gamma_t$ ,  $t = 0, \dots, T$ . This property however does not hold when using second-order Taylor or sigma-points approximations for the integrals appearing in (23), and the choice of  $\Gamma_t$  will then impact the performance of the algorithm (see, e.g., [Särkkä, 2013](#), Ch. 5-6, for the role of the reference covariance in classical Gaussian approximated filtering and smoothing).*

The linear approximations (21), together with the known (or approximated) first two moments  $m_0$  and  $P_0$  of  $\mathbb{P}_0$ , can then be used to form a proposal distribution defined as an auxiliary LGSSM smoothing distribution with density

$$q(z_{0:T} | u_{0:T}, x_{0:T}, y_{0:T}) \propto \mathcal{N}(z_0; m_0, P_0) \left\{ \prod_{t=0}^T \mathcal{N}(y_t; H_t z_t + c_t, R_t) \mathcal{N}\left(u_t; z_t, \frac{\delta}{2} \Sigma_t\right) \right\} \left\{ \prod_{t=1}^T \mathcal{N}(z_t; F_{t-1} z_{t-1} + b_{t-1}, Q_{t-1}) \right\}. \quad (24)$$

This proposal distribution is then included as part of a Metropolis–Rosenbluth–Teller–Hastings acceptance-rejection step. The resulting sampler then corresponds to [Algorithm 1](#).

Evaluating the augmented density (20) appearing in the acceptance ratio is easily done. Therefore, to effectively implement the steps above we only need to understand how to sample from the smoothing distribution of the LGSSM at hand, and compute the corresponding smoothing density  $\frac{q(x_{0:T}^*, y_{0:T}, u_{0:T} | x_{0:T})}{q(y_{0:T}, u_{0:T} | x_{0:T})}$ . This is readily achieved by applying sequential Kalman filtering equations to compute the filtering densities as well as the marginal likelihood of the true and auxiliary observations (see, e.g., [Särkkä, 2013](#), Chap. 4), and then sampling from the pathwise smoothing distribution backwards ([de Jong and Shephard, 1995](#)). We are therefore able to achieve an overall computational complexity of  $\mathcal{O}(T \times d_x^3)$ . This is to

---

**Algorithm 1:** General Auxiliary Kalman sampler
 

---

**Result:** An updated trajectory  $x_{0:T}$

```

1 Function AUXKALMANSAMPLER( $x_{0:T}$ )
  // Generate the auxiliary observations
2 for  $t = 0, 1, \dots, T$  sample  $u_t \mid x_t \sim \mathcal{N}(\cdot; x_t, \frac{\delta}{2}\Sigma_t)$ 
  // Proposal part
3 for  $t = 0 \dots, T$  do
4   if  $t > 0$  then
5     | Form an approximation  $\mathcal{N}(z_t; F_{t-1}^*z_{t-1} + b_{t-1}^*, Q_{t-1}^*) \approx p_t(z_t \mid z_{t-1})$  around  $x_{t-1}$ 
6     | Form an approximation  $\mathcal{N}(y_t; H_t^*z_t + c_t^*, R_t^*) \approx p_t(y_t \mid z_t)$ , around  $x_t$ 
7   Sample  $x_{0:T}^* \sim q(\cdot \mid y_{0:T}, u_{0:T}, x_{0:T})$  and compute  $L^* = \frac{q(x_{0:T}^*, y_{0:T}, u_{0:T} \mid x_{0:T})}{q(y_{0:T}, u_{0:T} \mid x_{0:T})}$ 
  // MRTH step
8   Form the reversed proposal  $q^*(x_{0:T} \mid y_{0:T}, u_{0:T}, x_{0:T}^*)$  following steps 5 and 6 around  $x_{0:T}^*$  and
     compute  $L = \frac{q^*(x_{0:T}, y_{0:T}, u_{0:T} \mid x_{0:T}^*)}{q^*(y_{0:T}, u_{0:T} \mid x_{0:T}^*)}$ 
9   With probability  $\min\left(1, \frac{p(x_{0:T}^*, y_{0:T}, u_{0:T})L}{p(x_{0:T}, y_{0:T}, u_{0:T})L^*}\right)$ , set  $x_{0:T} = x_{0:T}^*$ 
10  return  $x_{0:T}$ 

```

---

be compared with the  $\mathcal{O}(T^2 \times d_x^2)$  complexity of using the latent Gaussian samplers directly (Titsias and Papaspiliopoulos, 2018, Section 3.3) as well as with the  $\mathcal{O}(T^3 \times d_x^3)$  cost of forming their samplers in the first place. In particular, when the model at hand depends on a parameter  $\theta$  updating it will not increase the cost of the  $x_{0:T}$  sampling step, as opposed to the algorithms of Titsias and Papaspiliopoulos (2018). This property is critical for deriving computationally efficient samplers targeting the joint distribution of the parameters and latent states.

We end this section by noting that, while we assumed that the model at hand was a state-space model for consistency and ease of exposition, the method developed in this section can also be applied to the generalised Feynman–Kac model (4). To do so, it suffices to apply the first order linearisation of Section 2.2 to the likelihood term, and, independently, the GSLR approach of this section to the latent dynamics model. Similarly, the linearisation method used for the observation and transition need not be the same one, and the choice thereof is fully left to the user; for instance, if the likelihood is separable, we can use a Laplace approximation for the individual terms  $g_t$ , but still an extended linearisation for the transitions.

### 3 Parallel-in-time pathwise sampling for LGSSMs

While sampling from the pathwise smoothing distribution of a LGSSM is rather easy, it naturally has a computational complexity of  $\mathcal{O}(T)$  in the number of time steps. However, this can be improved by parallelisation. In this section, we present two different methods to sample from a LGSSM in logarithmic  $\mathcal{O}(\log(T))$  time. The methods are based on similar ideas as the parallel smoothing methods presented in Särkkä and García-Fernández (2021). One of the method uses a computational primitive called prefix-sum or associative scan (Blelloch, 1989), which generalises cumulative sums to other (associative) operators than addition, while the second one relies on a divide-and-conquer mechanism. It is worth noting that we expect the former to perform better, in particular due to its lower memory requirements, but the second one can be used more easily in distributed settings.

Putting aside the notations of the rest of the article, in this section we consider a generic LGSSM given by its joint distribution  $q(x_{0:T}, y_{0:T})$  over the states and observations such that

$$\begin{aligned}
 X_0 &\sim \mathcal{N}(m_0, P_0) \\
 X_t &= F_{t-1}X_{t-1} + b_{t-1} + e_{t-1}, \quad t > 0 \\
 Y_t &= H_t z_t + c_t + r_t, \quad t \geq 0,
 \end{aligned} \tag{25}$$

with  $e_t \sim \mathcal{N}(0, Q_t)$  and  $r_t \sim \mathcal{N}(0, R_t)$  for all  $t \geq 0$ .



### 3.1 Prefix-sum sampling for LGSSMs

We now describe how to sample from  $q(\cdot | y_{0:T})$  using similar methods as in [Särkkä and García-Fernández \(2021\)](#); [Yaghoobi et al. \(2021, 2022\)](#). Given that both the target of the log-likelihood (as a sum of  $T$  independent terms) and the marginal log-likelihood of the LGSSM approximation ([Särkkä and García-Fernández, 2021](#)) can be computed in  $\mathcal{O}(\log(T))$  on parallel hardware, this is the only missing piece for implementing a parallel-in-time version of our auxiliary Kalman samplers. While several different formulations (see, e.g., [Doucet, 2010](#); [Frühwirth-Schnatter, 1994](#)) may be employed to do so, we here focus on the forward filtering backward sampling (FFBS) ([Frühwirth-Schnatter, 1994](#)) approach.

We can compute the filtering distributions  $q(x_t | y_{0:t}) = \mathcal{N}(x_t; m_t, P_t)$  for (25) in parallel using the methods of [Särkkä and García-Fernández \(2021\)](#). Furthermore, we know (by adding a bias term to [Frühwirth-Schnatter, 1994](#), Proposition 1) that

$$\begin{aligned} q(x_T | y_{0:T}) &= \mathcal{N}(x_T; m_T, P_T) \\ q(x_t | x_{t+1}, y_{0:t}) &= \mathcal{N}(x_t; m_t + G_t x_{t+1} - F_t m_t - b_t, \Sigma_t), \quad t < T, \end{aligned} \quad (26)$$

where  $G_t = P_t F_t^\top (F_t P_t F_t^\top + Q_t)^{-1}$  and  $\Sigma_t = P_t - G_t (F_t P_t F_t^\top + Q_t) G_t^\top$  for all  $t < T$ .

We can furthermore rearrange the terms to express  $\hat{X}_t \sim q(x_t | \hat{X}_{t+1}, y_{0:t})$  recursively as

$$\hat{X}_t = G_t \hat{X}_{t+1} + \nu_t, \quad (27)$$

where all the  $\nu_t$ 's are independent, and  $\nu_t \sim \mathcal{N}(m_t - G_t(F_t m_t + b_t), \Sigma_t)$  for all  $t < T$ . We also let  $G_T = 0$ , so that we can then define  $\nu_T \sim \mathcal{N}(m_T, P_T)$ . Because the means and covariances of the  $\nu_t$ 's only depend on the LGSSM coefficients and the filtering means and covariances at time  $t$ , they can be sampled fully in parallel. To sample from  $q(x_{0:T} | y_{0:T})$  we then need to apply (27) to the pre-sampled sequence  $U_t \sim \nu_t$ ,  $t = 0, \dots, T$ . However, the recursive dependency in (27) is not directly parallelisable, and we instead need to rephrase it in terms of an associative operator, which will allow us to use prefix-sum primitives ([Blelloch, 1989](#)). Thankfully, this is readily done by considering the  $\circ$  operator defined as follows

$$\begin{aligned} (G_{ij}, U_{ij}) &= (G_i, U_i) \circ (G_j, U_j), \quad \text{where} \\ G_{ij} &= G_i G_j, \quad U_{ij} = G_i U_j + U_i. \end{aligned} \quad (28)$$

**Proposition 3.1.** *The backward prefix-sum of operator  $\circ$  applied to the sequence  $(G_t, U_t)$ ,  $t = 0, \dots, T$ , recovers the pathwise smoothing distribution  $q(x_{0:T} | y_{0:T})$ , that is, if  $(\tilde{G}_t, \tilde{U}_t) = (G_t, U_t) \circ \dots \circ (G_T, U_T)$ , then  $(\tilde{U}_0, \dots, \tilde{U}_T)$  is distributed according to  $q(x_{0:T} | y_{0:T})$ .*

*Proof.* The operator  $\circ$  defined in (28) is clearly associative. We prove that its result corresponds to sampling from the pathwise smoothing distribution by reversed induction: suppose that  $(\tilde{U}_t, \dots, \tilde{U}_T)$  is distributed according to  $q(x_{t:T} | y_{0:T})$ , then  $\tilde{U}_{t-1} = G_{t-1} \tilde{U}_t + U_{t-1}$ , which is distributed according to  $q(x_{t-1} | \tilde{U}_t, y_{0:t-1})$  as discussed before, so that  $(\tilde{U}_{t-1}, \dots, \tilde{U}_T)$  is distributed according to  $q(x_{t-1:T} | y_{0:T})$ . The initial case follows from the definition of  $U_T$ .  $\square$

To summarise, in order to perform prefix-sum sampling of LGSSMs, it suffices to use the parallel-in-time Kalman filtering method of [Särkkä and García-Fernández \(2021\)](#) to compute the filtering means and covariances  $m_t, P_t$ ,  $t = 0, \dots, T$ , then form all the elements  $G_t$  and sample  $U_t$  fully in parallel, and finally, apply the prefix-sum primitive ([Blelloch, 1989](#)) to  $(G_t, U_t)_{t=0}^T$  with the associative operator  $\circ$ .

### 3.2 Divide-and-conquer sampling for LGSSMs

We now present a divide-and-conquer alternative to Section 3.1 for PIT sampling from the pathwise smoothing distribution of LGSSMs. The method is based on recursively finding tractable Gaussian expressions for the ‘‘bridging’’  $q(x_l | y_{0:T}, x_k, x_m)$ ,  $0 \leq k < l < m \leq T$  of the smoothing distribution. This will allow us to derive a tree-based divide-and-conquer sampling mechanism for the pathwise smoothing distribution  $q(x_{0:T} | y_{0:T})$ .

Suppose we are given the LGSSM (25), then given three indices  $0 \leq k < l < m \leq T$ . We have

$$q(x_l | y_{0:T}, x_k, x_m) = \frac{q(x_k, x_l | y_{0:T}, x_m)}{q(x_k | y_{0:T}, x_m)} \quad (29)$$

with, furthermore,

$$q(x_k, x_l | y_{0:T}, x_m) = q(x_k | y_{0:T}, x_l) q(x_l | y_{0:T}, x_m) \quad (30)$$

thanks to the Markovian structure of the model. Now let  $q(x_k | y_{0:T}, x_l)$  and  $q(x_l | y_{0:T}, x_m)$  be given by

$$\begin{aligned} q(x_k | y_{0:T}, x_l) &= \mathcal{N}(x_k; E_{k:l}x_l + g_{k:l}, L_{k:l}) \\ q(x_l | y_{0:T}, x_m) &= \mathcal{N}(x_l; E_{l:m}x_m + g_{l:m}, L_{l:m}) \end{aligned} \quad (31)$$

for some parameters  $E_{k:l}$ ,  $g_{k:l}$ ,  $L_{k:l}$ ,  $E_{l:m}$ ,  $g_{l:m}$ , and  $L_{l:m}$  that we will define below. Then we can write

$$\begin{aligned} q(x_k, x_l | y_{0:T}, x_m) \\ = \mathcal{N}\left(\begin{pmatrix} x_l \\ x_k \end{pmatrix}; \begin{pmatrix} E_{l:m}x_m + g_{l:m} \\ E_{k:l}E_{l:m}x_m + E_{k:l}g_{l:m} + g_{k:l} \end{pmatrix}, \begin{pmatrix} L_{l:m} & L_{l:m}E_{k:l}^\top \\ E_{k:l}L_{l:m} & E_{k:l}L_{l:m}E_{k:l}^\top + L_{k:l} \end{pmatrix}\right) \end{aligned} \quad (32)$$

giving both the marginal distribution of  $x_k$

$$\begin{aligned} q(x_k | y_{0:T}, x_m) &= \mathcal{N}(x_k; E_{k:l}E_{l:m}x_m + E_{k:l}g_{l:m} + g_{k:l}, E_{k:l}L_{l:m}E_{k:l}^\top + L_{k:l}) \\ &= \mathcal{N}(x_k; E_{k:m}x_m + g_{k:m}, L_{k:m}), \end{aligned} \quad (33)$$

where

$$E_{k:m} = E_{k:l}E_{l:m}, \quad g_{k:m} = E_{k:l}g_{l:m} + g_{k:l}, \quad L_{k:m} = E_{k:l}L_{l:m}E_{k:l}^\top + L_{k:l}, \quad (34)$$

and (after simplification for (34)) the conditional distribution of  $x_l$

$$q(x_l | y_{0:T}, x_k, x_m) = \mathcal{N}(x_l; G_{k:l:m}x_k + \Gamma_{k:l:m}x_m + w_{k:l:m}, V_{k:l:m}), \quad (35)$$

for

$$\begin{aligned} G_{k:l:m} &= L_{l:m}E_{k:l}^\top L_{k:m}^{-1}, & w_{k:l:m} &= g_{l:m} - G_{k:l:m}g_{k:m}, \\ \Gamma_{k:l:m} &= E_{l:m} - G_{k:l:m}E_{k:m}, & V_{k:l:m} &= L_{l:m} - G_{k:l:m}L_{k:m}G_{k:l:m}^\top. \end{aligned} \quad (36)$$

This construction provides a recursive tree structure for sampling from  $q(x_{0:T} | y_{0:T})$  which can be initialised by

$$q(x_t | y_{0:T}, x_{t+1}) = \mathcal{N}(x_t; E_{t:t+1}x_{t+1} + g_{t:t+1}, L_{t:t+1}), \quad (37)$$

with

$$E_{t:t+1} = P_t F_t^\top (F_t P_t F_t^\top + Q_t)^{-1}, \quad g_{t:t+1} = m_t - E_{t:t+1}(F_t m_t + b_t), \quad L_{t:t+1} = P_t - E_{t:t+1}F_t P_t, \quad (38)$$

and  $q(x_T | y_{0:T}) = \mathcal{N}(x_T; m_T, P_T)$ . Finally, noting that

$$q(x_0 | y_{0:T}, x_T) = \mathcal{N}(x_0; E_{0:T}m_T + g_{0:T}, L_{0:T}), \quad (39)$$

we can combine these identities to form a divide-and-conquer algorithm.

To summarise, in order to perform divide-and-conquer sampling of LGSSMs, it suffices, as in Section 3.1, to use the parallel-in-time Kalman filtering method of Särkkä and García-Fernández (2021) to compute the filtering means and covariances  $m_t$ ,  $P_t$ ,  $t = 0, \dots, T$ . After this, we can recursively compute the tree of elements  $E_{k:m}$ ,  $g_{k:m}$ ,  $L_{k:m}$ , together with the auxiliary variables  $G_{k:l:m}$ ,  $w_{k:l:m}$ ,  $\Gamma_{k:l:m}$ ,  $V_{k:l:m}$ , starting from  $E_{t:t+1}$ ,  $g_{t:t+1}$ ,  $L_{t:t+1}$ , for  $t = 0, 1, \dots, T - 1$ , then  $E_{t-1:t+1}$ ,  $g_{t-1:t+1}$ ,  $L_{t-1:t+1}$ , for  $t = 1, 3, 5, \dots, 2\lfloor(T-1)/2\rfloor + 1$ , etc. Once this has been done, we can then sample from  $q(x_T | y_{0:T})$ , then from  $q(x_0 | y_{0:T}, x_T)$ , then  $x_{\lfloor T/2 \rfloor}$  conditionally on  $x_0$  and  $x_T$ , then, in parallel  $x_{\lfloor T/4 \rfloor}$  and  $x_{\lfloor 3T/4 \rfloor}$ , conditionally on the rest, and continue until all have been sampled.

## 4 Auxiliary particle Gibbs samplers

Most of the article so far has been concerned with MCMC algorithms using Kalman primitives to sample from a LGSSM proposal distribution designed as a local approximation of the target model at hand. This method, while expected to work particularly well when the prior is almost Gaussian and the potential relatively non-informative, presents at least three limitations: (i) it accepts or rejects a full trajectory at once, so that an unfortunate choice for a single time step would result in rejecting the full proposal, thereby hindering progress of the Markov chain; (ii) it requires that the full model be *de facto* differentiable or

has fully tractable moments, preventing its use in, for example, bounded state-spaces; (iii) it is hardly applicable to very non-Gaussian dynamics. For these reasons, in this section, we turn ourselves to the successful class of particle MCMC algorithms, in particular particle Gibbs algorithms, and show how the auxiliary observation trick can be leveraged to design efficient MCMC samplers for Feynman–Kac models. We first quickly recall the basic particle Gibbs algorithm, after which we show how it can be used to sample from an auxiliary target resembling (12). A general method is first presented, after which we show how additional information may be used to improve the sampler.

## 4.1 SMC and particle Gibbs algorithms

Particle Gibbs algorithms are Gibbs-like MCMC samplers that target the posterior distribution of Feynman–Kac models (Andrieu et al., 2010; Lindsten et al., 2012, 2014). In their simplest form, they consist in running a particle filter algorithm conditioned on the current state of the MCMC chain “surviving” the resampling step. This kernel, called conditional SMC (cSMC), can be proven to be ergodic for the pathwise smoothing distribution of the systems under the weak hypothesis that the potential functions are bounded above (Lee et al., 2020, and references within). In Algorithm 2, we reproduce the original version (Andrieu et al., 2010) of a cSMC kernel with  $N \geq 2$  particles, targeting the posterior distribution of a generic Feynman–Kac model  $\pi(x_{0:T}) \propto g_0(x_0) p_0(x_0) \left\{ \prod_{t=1}^T g_t(x_t, x_{t-1}) p_t(x_t | x_{t-1}) \right\}$ . This will serve as the basis for our discussion in the remainder of Section 4.

---

### Algorithm 2: Conditional SMC

---

**Result:** An updated trajectory  $x_{0:T}$

```

1 Function cSMC( $x_{0:T}, N$ )
   // Forward propagation
2 for  $n = 1, 2, \dots, N - 1$  do
3   | Sample  $X_0^n \sim p_0$  and set  $w_0^n = g_0(X_0^n)$ 
4   | Set  $X_0^N = x_0, w_0^N = g_0(X_0^N)$ 
5   for  $t = 1, \dots, T$  do
6     | for  $n = 1, \dots, N - 1$  do
7       | | Sample  $A_t^n$  with  $\mathbb{P}(A_t^n = k) \propto w_{t-1}^k$ 
8       | | Sample  $X_t^n \sim p_t(\cdot | X_{t-1}^{A_t^n})$  Set  $w_t^n = g_t(X_t^n | X_{t-1}^{A_t^n})$ 
9       | | Set  $X_t^N = x_t, w_t^N = g_t(x_t | x_{t-1})$ 
   // Genealogy selection
10  | Sample  $B_T$  with  $\mathbb{P}(B_T^n = k) \propto w_T^k$  and set  $x_T = X_T^{B_T}$ 
11  for  $t = T - 1, \dots, 0$  do
12  | | Set  $B_t = A_{t+1}^{B_{t+1}}, x_t = X_t^{B_t}$ 
13  return  $x_{0:T}$ 

```

---

Other versions of this algorithm exist, in particular, when it is possible to evaluate  $p_t$  pointwise, we can rejuvenate the selection of the genealogy, allowing for lower degeneracy in the early time steps. The most notable two such methods are the backward and ancestor sampling methods (Whiteley, 2010; Lindsten et al., 2014, respectively). Another method, useful in our context, is that of Corenflos et al. (2022, Section 3), which implements a parallel-in-time conditional SMC, particularly amenable to when the dynamics model is separable, that is, when  $p_t(x_t | x_{t-1}) = p_t(x_t)$  does not depend on  $x_{t-1}$  as will be the case in the next section.

## 4.2 Particle Gibbs for Feynman–Kac models with auxiliary observations

Section 2 offers a class of new samplers for latent dynamical systems with tractable moments. It is however not the case that all practical problems verify this assumption, or that the potential function is always differentiable. In this section, we instead consider the case of Feynman–Kac models (6) with tractable densities. For this class of models, the auxiliary target corresponds to a model with an augmented potential function

$$\pi(x_{0:T}, u_{0:T}) \propto g_0(x_0) p_0(x_0) \left\{ \prod_{t=1}^T g_t(x_t, x_{t-1}) p_t(x_t | x_{t-1}) \right\} \left\{ \prod_{t=0}^T \mathcal{N} \left( u_t; x_t, \frac{\delta}{2} \Sigma_t \right) \right\}. \quad (40)$$

In order to sample from  $\pi(x_{0:T}, u_{0:T})$ , it is therefore enough to implement an abstract algorithm given by Algorithm 3.

---

**Algorithm 3:** Auxiliary cSMC

---

**Result:** An updated trajectory  $x_{0:T}^{k+1}$

- 1 **Function** AUX-CSMC( $x_{0:T}^k$ )
- 2     **for**  $t = 0, 1, \dots, T$  **sample**
- 3     |      $u_t \sim \mathcal{N}(\cdot; x_t^k, \frac{\delta}{2}\Sigma_t)$
- 4     |     Sample  $x_{0:T}^{k+1} \sim K(\cdot | x_{0:T}^k)$  // from a cSMC kernel keeping  $\pi(x_{0:T} | u_{0:T}^{k+1})$  invariant
- 5     **return**  $x_{0:T}^{k+1}$

---

Clearly, in Algorithm 3, if  $(x_{0:T}^k, u_{0:T}^k)$  are distributed according to  $\pi$ , then  $(u_{0:T}^{k+1}, x_{0:T}^k)$  are too after line 3, so that  $x_{0:T}^k$  is distributed according to  $\pi(\cdot | u_{0:T}^{k+1})$ , and therefore  $(x_{0:T}^{k+1}, u_{0:T}^{k+1})$  are still distributed according to  $\pi$  after line 4. Otherwise said, this algorithm can be seen as a “true” particle Gibbs algorithm (Andrieu et al., 2010) for the choice of an improper prior  $\pi(u_{0:T}) = 1$  for the auxiliary variables.

At first sight this may seem like a very bad idea, and it appears like we have made the problem more difficult than it was originally, and this is probably the reason why (to the best of our knowledge) this has not been *explicitly* proposed before. Indeed, instead of considering the potential function  $g_t(x_t, x_{t-1})$ , we are now considering the potential function  $g_t(x_t, x_{t-1}) \mathcal{N}(u_t; x_t, \frac{\delta}{2}\Sigma_t)$  at each time step  $t$ . This new potential function becomes very informative as  $\delta$  gets smaller, which is known to induce high variance weights in particle filtering and smoothing algorithms (see, e.g. Chopin and Papaspiliopoulos, 2020, Section 10.3.1). However, rather than seeing  $\mathcal{N}(u_t; x_t, \frac{\delta}{2}\Sigma_t)$  as describing an auxiliary observation, we can leverage the symmetry of Gaussian distributions to look at it as the generative model  $\mathcal{N}(x_t; u_t, \frac{\delta}{2}\Sigma_t)$  instead. We can consider the model

$$\pi(x_{0:T}, u_{0:T}) \propto \tilde{p}_0(x_0) \left\{ \prod_{t=1}^T \tilde{p}_t(x_t | x_{t-1}) \right\} \tilde{g}_0(x_0) \left\{ \prod_{t=1}^T \tilde{g}_t(x_t, x_{t-1}) \right\}, \quad (41)$$

for the modified dynamics  $\tilde{p}_t(x_t | x_{t-1}) = \mathcal{N}(x_t; u_t, \frac{\delta}{2}\Sigma_t)$  and potential functions  $\tilde{g}_t = g_t \cdot p_t$ ,  $t = 0, 1, \dots, T$ . This change of perspective immediately makes the problem much simpler, as we are now given a model with an informative and separable prior for which we can implement Step 4 of Algorithm 3 via Algorithm 2. Moreover, because the auxiliary prior model is separable across time, the method of Corenflos et al. (2022) applies directly<sup>3</sup>, and a parallel-in-time particle Gibbs can be implemented to reduce the computational complexity to  $\mathcal{O}(\log T)$  on parallel hardware. We also note that, contrarily to Corenflos et al. (2022, Section 5.2), in this specific case, doing so would not necessarily come at a loss of statistical efficiency compared to sequential conditional SMC counterparts. This is due to the fact that the sequential algorithms would also rely on sampling from independent proposals.

In hindsight, it is easy to see that this method is *exactly* the same one as the one proposed in Finke and Thiery (2023, Algorithm 3 and extensions) who instead phrase it as a form of conditional SMC with exchangeable proposals. Informally, rather than using a proposal  $\tilde{p}_t(x_t | x_{t-1})$ , they use a proposal  $\tilde{p}_t(x_t^1, \dots, x_t^N)$  which induces an exchangeable dependency across particles, that is,  $\tilde{p}_t(x_t^1, \dots, x_t^N) = \tilde{p}_t(x_t^{\sigma(1)}, \dots, x_t^{\sigma(N)})$  for any permutation  $\sigma$ . As done in Finke and Thiery (2023) – and first introduced in the context of classical MCMC in Tjelmeland (2004) –, in the case of Gaussians, taking a conditional sample  $p(\dots, x_t^{k-1}, x_t^k, \dots | x_t^k)$  can for instance be achieved by first sampling a “centering” variable  $u_t \sim \mathcal{N}(x_t^k, \frac{\delta}{2}I)$  and then the remainder of the variables from  $\prod_{i \neq k} \mathcal{N}(x_t^i; u_t, \frac{\delta}{2}I)$ . This directly corresponds to Algorithm 3 for the modified Feynman–Kac model (41).

**Proposition 4.1.** *The algorithms of Finke and Thiery (2023) implement Algorithm 3 with separable proposal distributions  $\mathcal{N}(\cdot; u_t, \frac{\delta}{2}\Sigma_t)$  for different choices of kernels  $K$ : embedded HMM (Neal, 2003), conditional SMC (Andrieu et al., 2010), conditional SMC with forced move (Chopin and Singh, 2015), and conditional SMC with backward sampling (Whiteley, 2010).*

They show that, for a given choice of a standard conditional SMC – with and without backward sampling – Algorithm 3 avoids the curse of dimensionality, that is, its mixing time increases linearly with respect to  $d_x$  rather than exponentially. This new perspective on their method is rich in consequences:

---

<sup>3</sup>While in Corenflos et al. (2022) it was derived for likelihood terms  $g_t(x_t)$  rather than  $g_t(x_t, x_{t-1})$  this was a notational simplification, and all the results derived within in fact hold for bivariate potentials.

the entirety of the literature on particle Gibbs can be applied to step 4 of Algorithm 3, and we can expect that the curse of dimensionality can be controlled in this case too.

For instance, while the parallelisation in time of our method via Corenflos et al. (2022) is immediate given its “pure” particle Gibbs interpretation, it was not directly obvious (although likely) that it applied to the perspective of Finke and Thiery (2023, Propositions 4.1, 4.2, and 4.3). In the following section, we see how we can further extend this new perspective on the algorithm of Finke and Thiery (2023) to develop statistically superior local particle Gibbs samplers.

### 4.3 Adapted proposals in particle Gibbs with auxiliary observations

In the previous section, we have described an algorithm that recovers Finke and Thiery (2023, Algorithm 3 and extensions). However, explicitly introducing the auxiliary variable allows us to decouple the state of the Markov chain and the generative model, so that we can incorporate statistical information in the auxiliary particle Gibbs sampler beside simple locality. Formally, we can implement “locally adapted” particle filters for  $\pi(x_{0:T} | u_{0:T})$  to be used in the forward pass of Algorithm 2. While this can be applied to many models, we demonstrate how this can be done for differentiable models and for those that have (approximately) conditional Gaussian transitions and arbitrary potential functions.

When the potential functions  $g_t$  are differentiable, it is possible to incorporate first or second order information from the potential. Indeed, for  $g_t = \exp(\gamma_t)$  and  $g = \prod_{t=0}^T g_t = \exp(\gamma)$ , we have

$$\begin{aligned} g(x_{0:T}) &= \exp(\gamma(x_{0:T})) \\ &\approx \exp\left(\gamma(u_{0:T}) + \sum_{t=0}^T \frac{\partial \gamma(u_{0:T})}{\partial x_t} \cdot (x_t - u_t)\right) =: \prod_{t=0}^T \hat{g}_t(x_t | u_{0:T}). \end{aligned} \quad (42)$$

Now, similarly to Section 2, we can form the proposal distributions

$$\begin{aligned} \tilde{p}_t(x_t | x_{t-1}, u_{0:T}) &\propto \mathcal{N}(x_t; u_t, \frac{\delta}{2}\Sigma_t) \hat{g}_t(x_t | u_{0:T}) \\ &\propto \mathcal{N}\left(x_t; u_t + \frac{\delta}{2}\Sigma_t \frac{\partial \gamma(u_{0:T})}{\partial x_t}, \frac{\delta}{2}\Sigma_t\right) \end{aligned} \quad (43)$$

and similarly for  $\tilde{p}_0$ . Finally, when  $p_t$  is also differentiable, we can also include information from it in the sampler by considering  $\exp(\gamma) = \prod_{t=0}^T p_t g_t$  rather than simply using  $g_t$ . Interestingly, these new proposal distributions are separable in time, so that they can be used in the parallel-in-time particle Gibbs algorithm of Corenflos et al. (2022) at no additional cost.

When the conditional mean and covariances of the prior process are available, as in Section 2.2, we can easily design a model (this is called a guided proposal in Chopin and Papaspiliopoulos, 2020, Section 10.3.2) locally adapted to the auxiliary observation:

$$\begin{aligned} \tilde{p}_t(x_t | x_{t-1}, u_t) &\propto \mathcal{N}\left(u_t; x_t, \frac{\delta}{2}\Sigma_t\right) \mathcal{N}\left(x_t; m_{t-1}^X(x_{t-1}), C_{t-1}^X(x_{t-1})\right) \\ &\propto \mathcal{N}(x_t; \mu_t, \Lambda_t), \end{aligned} \quad (44)$$

where  $K_{t-1} = C_{t-1}^X(x_{t-1}) [C_{t-1}^X(x_{t-1}) + \frac{\delta}{2}\Sigma_t]^{-1}$ ,  $\mu_t = m_{t-1}^X(x_{t-1}) + K_{t-1}[u_t - m_{t-1}^X(x_{t-1})]$ , and  $\Lambda_t = C_{t-1}^X(x_{t-1}) - K_{t-1}C_{t-1}^X(x_{t-1})$ . A similar form is available for  $p_0$ . Using this new proposal, an equivalent Feynman–Kac model will then take the form

$$\pi(x_{0:T} | u_{0:T}) \propto \tilde{p}_0(x_0) \left\{ \prod_{t=1}^T \tilde{p}_t(x_t | x_{t-1}) \right\} \tilde{g}_0(x_0) \left\{ \prod_{t=1}^T \tilde{g}_t(x_t, x_{t-1}) \right\}, \quad (45)$$

where  $\tilde{p}$  is given by (44), and

$$\tilde{g}_0(x_0) = \frac{g_0(x_0)p_0(x_0)}{\tilde{p}_0(x_0)} \mathcal{N}\left(u_0; x_0, \frac{\delta}{2}\Sigma_0\right), \quad \tilde{g}_t(x_t, x_{t-1}) = \frac{g_t(x_t, x_{t-1})p_t(x_t | x_{t-1})}{\tilde{p}_t(x_t | x_{t-1})} \mathcal{N}\left(u_t; x_t, \frac{\delta}{2}\Sigma_t\right). \quad (46)$$

Using such a generative model, contrary to the independent auxiliary proposal cases, is not parallelisable in time, and will scale as  $\mathcal{O}(T)$ , even on parallel hardware. On the other hand, when the potential is weakly informative compared to the dynamics, we can expect them to have better statistical properties, in the sense that they are likely to have lower autocorrelation than their independent proposal

counterparts. We also note that the construction proposed in (44) and (45) extends to other methods developed to leverage approximate Gaussian conjugacy relationships in state-space models, for instance, they are directly compatible to Laplace approximations of the potential function (see, e.g. [Chopin and Papaspiliopoulos, 2020](#), Section 10.5.3) or Rao–Blackwellisation ([Murphy and Russell, 2001](#)).

Finally, it is worth highlighting that the two approaches presented in this section are not mutually exclusive. Indeed, we can combine an approximately Gaussian transition model together with a differentiable potential to obtain hybrid adapted proposals that may work better than their individual components taken in isolation. With the notations above, this would, for example, correspond to

$$\begin{aligned} \tilde{p}_t(x_t | x_{t-1}, u_t) &\propto \mathcal{N}\left(u_t; x_t, \frac{\delta}{2}\Sigma_t\right) \mathcal{N}\left(x_t; m_{t-1}^X(x_{t-1}), C_{t-1}^X(x_{t-1})\right) \hat{g}_t(x_t | u_{0:T}) \\ &\propto \mathcal{N}\left(u_t + \frac{\delta}{2}\Sigma_t \frac{\partial \gamma(u_{0:T})}{\partial x_t}; x_t, \frac{\delta}{2}\Sigma_t\right) \mathcal{N}\left(x_t; m_{t-1}^X(x_{t-1}), C_{t-1}^X(x_{t-1})\right), \end{aligned} \quad (47)$$

if the linearisation point of  $\gamma$  was taken to be  $u_{0:T}$ .

Other linearisation/combination choices are possible, and the willing statistician is free to fully leverage the flexibility brought by introducing the auxiliary observations  $u_{0:T}$ . Understanding which is the best choice will typically be application specific, although we expect the methods presented in this section to provide a competitive test-bed for more advanced methods.

#### 4.4 Extension to pseudo-marginal methods

While the particle Gibbs approach to sampling from (40) is perhaps the most natural, it is also possible to instead consider a pseudo-marginal approach ([Andrieu and Roberts, 2009](#)) as given by the particle marginal Metropolis–Hastings (PMMH) sampler of [Andrieu et al. \(2010\)](#). Consider a proposal distribution  $q(du'_{0:T} | u_{0:T})$ , for example,  $\prod_0^T \mathcal{N}(u'_t; u_t, \frac{\delta}{2}\Sigma_t)$ . Similarly to PMMH, because sequential Monte Carlo provides an unbiased estimate  $\hat{\mathcal{Z}}_N(u_{0:T})$  of the normalising constant for  $\pi(x_{0:T} | u_{0:T})$ , we can marginally target  $\pi(x_{0:T})$  using a PMMH methodology. We succinctly summarise this extension in Algorithm 4.

---

##### Algorithm 4: Auxiliary pseudo-marginal sampler

---

**Result:** An updated trajectory  $x_{0:T}^{k+1}$

- 1 **Function** AUX-PM( $x_{0:T}^k, u_{0:T}^k, \hat{\mathcal{Z}}_N^k$ )
- 2   Sample  $u'_{0:T} \sim q(\cdot | u_{0:T}^k)$
- 3   Sample  $x'_{0:T}$  and  $\hat{\mathcal{Z}}'_N$  using a particle filter targeting  $\pi(x_{0:T} | u'_{0:T})$
- 4   Set  $x_{0:T}^{k+1}$  to  $x'_{0:T}$  with probability  $\frac{\hat{\mathcal{Z}}'_N q(u_{0:T}^k | u'_{0:T})}{\hat{\mathcal{Z}}_N^k q(u'_{0:T} | u_{0:T}^k)}$ , otherwise, set it to  $x_{0:T}^k$
- 5   **return**  $x_{0:T}^{k+1}$

---

This method is related to the correlated pseudo-marginal method of [Deligiannidis et al. \(2018\)](#), which instead considers the extended distribution

$$\pi(x_{0:T}, u_{0:T}) \propto g_0(x_0)p_0(x_0) \left\{ \prod_{t=1}^T g_t(x_t, x_{t-1}) p_t(x_t | x_{t-1}) \right\} \left\{ \prod_{t=0}^T \mathcal{N}(u_t; 0, I) \right\}, \quad (48)$$

where the  $u_t$ s represent Gaussian variables used to generate particles (and sample from the ancestors) within the sequential Monte Carlo routine. By correlating these over time, they show that the pseudo-marginal algorithm can be made to scale better with time series of increasing lengths  $T$ . This is because it results in correlated likelihood ratios  $\frac{\hat{\mathcal{Z}}'_N}{\hat{\mathcal{Z}}_N^k}$  which exhibit lower variance than they would have otherwise.

By using a proposal distribution adapted to the auxiliary target at hand, in a similar spirit as for the auxiliary particle Gibbs sampler of Algorithm 3, we can hope to also benefit from a reduced variance of the likelihood estimates ratio in Algorithm 4. This, however, is not because the two estimates are correlated, but rather because they will both exhibit lower variance individually than their non-augmented counterparts. Contrary to [Deligiannidis et al. \(2018\)](#), this method necessitates evaluation of the full (unnormalised) density of the Feynman–Kac model at hand, and will likely not perform well for a very large  $T$ . On the other hand, and in contrast to the correlated pseudo-marginal method ([Deligiannidis et al., 2018](#), see the comments in Theorem 3 and Section 5.3), Algorithm 4 is likely to perform well in higher dimensions, due to the localisation of the proposals. We leave the study of this question open for future work and focus on the auxiliary particle Gibbs algorithm in the remainder of this article.

## 5 Experimental evaluation

In this section, we aim to empirically evaluate the statistical and computational behaviours of our proposed methods. To this end, we consider three sets of examples.

- The first model performs joint parameter and state estimation for a discretely observed stochastic differential equation. This model was used in [Mider et al. \(2021\)](#) to assess the performance of their forward-guiding backward-filtering method. We demonstrate here how to use auxiliary samplers for the same purpose and show the competitiveness of our approach.
- The second one is a multivariate stochastic volatility model known to be challenging for Gaussian approximations and used as a benchmark in, for example, [Guarniero et al. \(2017\)](#); [Finke and Thiery \(2023\)](#). This model has latent Gaussian dynamics, and an observation model which happen to both be differentiable with respect to the latent state, so that all the methods of Section 2.2 and Section 4 apply. We consider the same parametrisation as in [Finke and Thiery \(2023\)](#), which makes the system lack ergodicity and the standard particle Gibbs samplers not converge.
- The last one is a spatio-temporal model with independent latent Gaussian dynamics and is used in [Crucinio and Johansen \(2022\)](#) as a benchmark for high dimensional filtering. This model is akin to a type of dynamic random effect model in the sense that the latent states only interact at the level of the observations. This model is used to illustrate how latent structure can be used to design computationally efficient Kalman samplers that beat cSMC ones when runtime is taken into account.

Throughout this section, when using an auxiliary cSMC sampler, be it the sequential or the parallel-in-time formulation, we use  $N = 25$  particles, and a target acceptance rate of 25% across all time steps. This is more conservative than the recommendation of [Finke and Thiery \(2023\)](#), corresponding to  $1 - (1 + N)^{-1/3} \approx 66\%$ . The difference stems from the fact that it may happen that the methods do not reach the relatively high acceptance rate implied by the more optimistic target for all time steps, even with very small  $\delta$  values. As a consequence, the sampler is “stuck” by only proposing very correlated trajectories in some places. This is mostly due to the largely longer time series considered here. Softening this resulted in empirically better mixing. Furthermore, for all the experiments, and following [Titsias and Papaspiliopoulos \(2018\)](#); [Finke and Thiery \(2023\)](#), we consider  $\delta\Sigma_t = \delta_t I$ , with  $\delta_t$  being constant across time steps for the Kalman samplers. Choosing a specific form for  $\Sigma_t$  is akin to pre-conditioning and is left for future works. We then calibrate  $\delta_t$  to achieve the desired acceptance rate (globally for Kalman samplers or per time step for the cSMC samplers) and the actual acceptance rate is reported in the relevant sections.

The implementation details for all the experiments are as follows: whenever we say that a method was run on a CPU, we have used an AMD<sup>®</sup> Ryzen Threadripper 3960X with 24 cores, and whenever the method has been run on a GPU, we used a Nvidia<sup>®</sup> GeForce RTX 3090 GPU with 24GB memory. All the experiments were implemented in Python ([Van Rossum and Drake, 2009](#)) using the JAX library ([Bradbury et al., 2018](#)) which natively supports CPU and GPU backends as well as automatic differentiation that we use to compute all the gradients we required. The code to reproduce the experiments listed below can be found at the following address: <https://github.com/AdrienCorenflos/aux-ssm-samplers>.

### 5.1 Parameter estimation in a continuous-discrete diffusion smoothing problem

In this section, we consider the same experiment as in [Mider et al. \(2021, Section 6.1\)](#), which consists in joint sampling of the state of a discretely observed chaotic Lorenz stochastic differential equation, and of the parameter defining its drift. The SDE is given, conditionally on a parameter  $\theta = (\theta_1, \theta_2, \theta_3)$  as a three-dimensional SDE  $dx = \beta_\theta(x) dt + \sigma dW_t$ , where  $W$  is a three-dimensional standard Wiener process and

$$\beta_\theta(x) = \begin{pmatrix} \theta_1(x_2 - x_1) \\ \theta_2 x_1 - x_2 - x_1 x_3 \\ x_1 x_2 - \theta_3 x_3 \end{pmatrix}. \quad (49)$$

The state is then observed at regular intervals (every  $t_0 = 0.01, t_1 = 0.02, \dots, t_K = 2$ ) through its second and third component only, giving an observation model  $Y_k \sim \mathcal{N}(Hx(t_k), 5I_2)$ , for  $H = \begin{pmatrix} 0 & 1 & 0 \\ 0 & 0 & 1 \end{pmatrix}$ . In order to provide comparable results to [Mider et al. \(2021\)](#), we use the code they provided to generate

|             | This paper | Mider et al. (2021) |
|-------------|------------|---------------------|
| $X_{1,1.5}$ | 31254.0    | 10480.3             |
| $X_{2,1.5}$ | 35469.9    | 22890.5             |
| $X_{3,1.5}$ | 36584.7    | 24070.2             |
| $\theta_1$  | 11850.0    | 4592.4              |
| $\theta_2$  | 22960.5    | 15379.5             |
| $\theta_3$  | 12240.5    | 10917.7             |

Table 1: Effective sample size (ESS) for the auxiliary sampler, computed using chains of length  $10^5$ . The results for Mider et al. (2021) are reported for ease of comparison.

the same dataset, and pick the same parametrisation of the model, including the same prior for the parameters. The Markov chain is then initialised according to the prior dynamics conditionally on the same initial parameter values as in Mider et al. (2021). As per their experiment, we sample from the joint distribution  $\pi(x(t'_0), \dots, x(t'_L), \theta \mid y_{0:K})$ , where  $t'_0 = 0, t'_1 = 2e - 4, \dots, t'_L = 2$  is a finer grid, making for a total sampling space dimension of  $3 + 30\,000$ . To do so, we too use the conjugacy relationship of  $\theta$  given the full path for  $x$ , implementing a Hastings-within-Gibbs routine which samples  $\theta$  conditionally on  $x(t'_0), \dots, x(t'_L)$  using its closed-form Gaussian posterior Mider et al. (2021, Proposition 4.5), and then the auxiliary Kalman sampler to sample  $x(t'_0), \dots, x(t'_L)$  conditionally on  $\theta$ .

In our case, because the observation model is linear, we use the following proposal in the Kalman sampler: first, given the current trajectory  $(x^k(t'_l))_{l=0}^L$  and parameter  $\theta^k$  state of the MCMC chain we linearise  $\mathbb{E}[x(t'_l) \mid x(t'_{l-1})] = \beta_{\theta^k}(x(t'_{l-1}))(t'_l - t'_{l-1})$  around  $x^k(t'_{l-1})$  using the method of Section 2.2 with extended linearisation, obtaining approximations  $p(x(t'_l) \mid x(t'_{l-1})) \approx \mathcal{N}(x(t'_l); F_{l-1}x(t'_{l-1}) + b_{l-1}, Q_{l-1})$ . For  $l = 0, \dots, L$  we then sample  $u_l \sim \mathcal{N}(x(t'_l), \frac{\delta}{2}I_3)$ , and then form the proposal

$$q((z(t'_l))_{l=0}^L \mid u_{0:L}, (x^k(t'_l))_{l=0}^L, y_{0:L}) \propto \mathcal{N}(z(t'_0); m_0, P_0) \left\{ \prod_{l=1}^L \mathcal{N}(z(t'_l); F_{l-1}z(t'_{l-1}) + b_{l-1}, Q_{l-1}) \right\} \left\{ \prod_{k=0}^K \mathcal{N}(y_k; Hz(t_k), 5I_2) \right\} \left\{ \prod_{l=0}^L \mathcal{N}(u_l; z(t'_l), \frac{\delta}{2}I_3) \right\} \quad (50)$$

targeting the augmented model

$$\pi((z(t'_l))_{l=0}^L \mid u_{0:L}, y_{0:K}) \propto \mathcal{N}(z(t'_0); m_0, P_0) \left\{ \prod_{l=1}^L p(z(t'_l) \mid z(t'_{l-1})) \right\} \left\{ \prod_{k=0}^K \mathcal{N}(y_k; Hz(t_k), 5I_2) \right\} \left\{ \prod_{l=0}^L \mathcal{N}(u_l; z(t'_l), \frac{\delta}{2}I_3) \right\}. \quad (51)$$

We run 2 500 adaptation steps, during which we modify  $\delta$  to target an average acceptance rate of 23.4% (as per Mider et al. (2021)). Interestingly, our actual acceptance rate after adaptation was closer to 70%, and the resulting  $\delta$  virtually infinite. This means that the proposal distribution is almost reversible with respect to the target distribution. This high acceptance rate did not negatively impact the convergence of our algorithm. In fact, our resulting effective sampling size was larger than the best one reported by Mider et al. (2021) for both the parameters and the smoothing marginals (while the posterior distributions were similar). We report this in Table 1.

In practice, our sampler took 3 149 seconds (52 minutes) to run on the GPU, and 9 424 seconds (2h30mn) on the CPU. Mider et al. (2021), on the other hand, report much faster run times (roughly 3-4 minutes). While this difference may seem massive, it can be imputed in totality to the difference in software for this experiment. Indeed, because they too rely on Gaussian filtering, the theoretical serial complexity of the two methods (when run on CPU) are exactly the same. While they use the programming language Julia (Bezanson et al., 2017), we use the JAX library (Bradbury et al., 2018) written in the Python language. Our choice comes with the benefit of direct GPU support, but also presents the inconvenience of not supporting varying size arrays. Consequently, rather than running Kalman filtering on the proposal LGSSM (50) optimally by alternatively considering independent observations of size 3 ( $u_l$ ) and 2 ( $y_k$ ), we have to consider stacked observations  $(u_l, y'_l)$  of dimension 5 and treat the  $y'_l$  as being missing when  $t'_l$  is not part of the  $t'_k$ . This technical limitation would be removed by considering instead a specialised implementation in a framework allowing for such optimisations.



## 5.2 Multivariate stochastic volatility model

We now consider the same multivariate stochastic volatility example as in [Finke and Thiery \(2023, Section E.3\)](#). This model is classically used as a benchmark for high dimensional SMC related methods (see also [Guarniero et al., 2017](#)). It is given by homogeneous auto-regressive Gaussian latent dynamics

$$p_t(x_t | x_{t-1}) = \mathcal{N}(x_t; F x_{t-1}, Q) \quad (52)$$

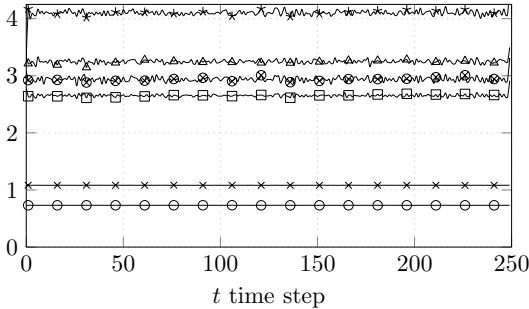
and a potential defined as a multidimensional observation model

$$g(x_{0:T}) = \prod_{t=0}^T h(y_t | x_t), \text{ where } h(y_t | x_t) = \prod_{d=1}^{d_x} \mathcal{N}(y_t(d); 0, \exp(x_t(d))). \quad (53)$$

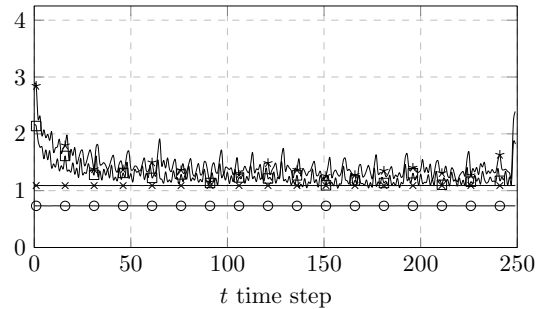
As per [Finke and Thiery \(2023\)](#), we take  $F = \phi I_d$ ,  $Q_{ij} = \tau(\delta(i=j) + \delta(i \neq j)\rho)$  for  $\phi = 90\%$ ,  $\tau = 2$ , and  $\rho = 25\%$ . Similarly, the initial distribution  $p_0(x_0)$  is also taken to be the stationary distribution of the latent Gaussian dynamics and we take  $d_x = 30$ . However, we increase the number of time steps to  $T = 250$ , rather than 50 and we take the number of particles for all the auxiliary cSMC algorithms to be  $N = 25$ .

The different methods we compare here are the following: (i) auxiliary Kalman sampler with first order linearisation (14) (both on CPU and GPU), (ii) with second order linearisation (16) (both on CPU and GPU), (iii) auxiliary cSMC sampler with backward sampling for the proposals  $\mathcal{N}(\cdot; u_t, \frac{\delta}{2}I)$  corresponding to [Finke and Thiery \(2023\)](#) (on CPU), (iv) auxiliary cSMC sampler with parallel-in-time ([Corenflos et al., 2022](#)) sampling for the proposals  $\mathcal{N}(\cdot; u_t, \frac{\delta}{2}I)$  (on GPU), (v) auxiliary cSMC sampler with backward sampling for the gradient-informed proposals (43) (on CPU), (vi) auxiliary cSMC sampler with parallel-in-time sampling for the gradient-informed proposals (43) (on GPU), and (vii) the guided auxiliary cSMC sampler with backward sampling for both the proposals (44) and (47) (on CPU).

In order to compare the samplers on this example, we generate 10 different datasets. For every dataset, we run each sampler for 2500 adaptation steps. After this, we run 10000 more iterations to compute the empirical root expected squared jump distance (RESJD, [Pasarica and Gelman, 2010](#)) for each sampler, defined as, for each time step  $t$ , the empirical value of  $\sqrt{\frac{1}{L} \sum_{l=1}^{L-1} \sum_{i,j=1}^d [X_{t+1}^{A+l+1}(i,j) - X_{t+1}^{A+l}(i,j)]^2}$ . All samplers, in both the sequential and parallel case were targeting 50% acceptance rate across all time steps and the effective acceptance rate ranged between 47 and 52% for all samplers and time steps. The averaged (across the 10 experiments) RESJD is reported in [Figure 1a](#) for the sequential versions of the algorithm, and in [Figure 1b](#) for the parallel counterparts (noting that there is, as expected, no statistical difference between the sequential and parallel implementations of the Kalman samplers). As highlighted



(a) Average root expected squared jump distance per iteration for the sequential versions of the auxiliary first order Kalman sampler  $\circ$ , second order Kalman sampler  $\times$ , cSMC sampler  $\square$ , gradient-informed cSMC  $*$  sampler, the guided cSMC  $\diamond$  sampler, and the gradient-informed guided cSMC  $\triangle$  sampler.

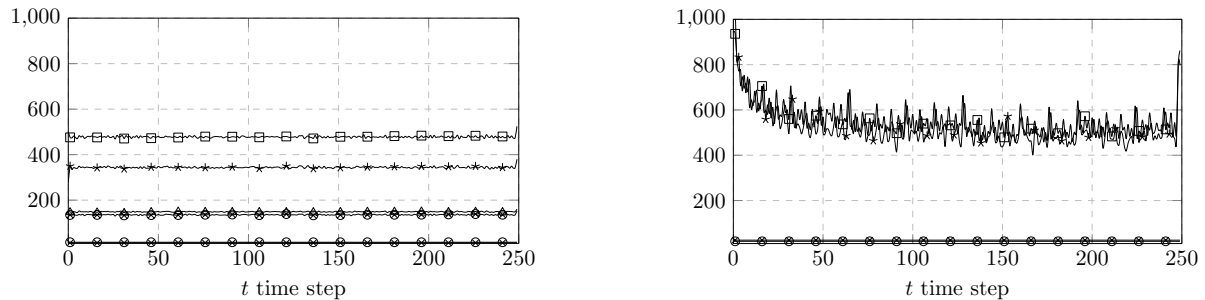


(b) Average root expected squared jump distance per iteration for the parallel versions of the auxiliary first order Kalman sampler  $\circ$ , second order Kalman sampler  $\times$ , cSMC sampler  $\square$ , and gradient-informed cSMC  $*$  sampler. The latter two are hard to distinguish, but the gradient-informed cSMC is generally above the non-informed.

Figure 1: Average (across 10 different experiments) root expected squared jump distance per iteration for all the sampler considered on the stochastic volatility model of Section 5.2. The results are split between CPU [1a](#) (where the classical sequential implementation of the cSMC with backward sampling was used) and GPU [1b](#) (where the parallel-in-time cSMC was used).

by Figure 1a, the gradient-informed auxiliary cSMC statistically dominates the alternatives for all time steps on both CPU and GPU (although this is less obvious on the GPU).

This picture, however, is modified when looking at the RESJD per second – heuristically corresponding to the average cumulative distance travelled by the sampler in a unit of time – rather than per iteration in Figures 2a and 2b. In this case, on the CPU, the method of Finke and Thiery (2023) dominates the other ones. This is because it offers reasonable statistical efficiency ( $\sim 70\%$  the RESJD of the most efficient sampler tested here) with a rather small time-complexity overall (no gradient calculation, and no matrix inversion like in the Kalman samplers is needed here). On the other hand, the Kalman samplers are here completely dominated by all Monte Carlo alternatives. The GPU picture is more mixed, and both the gradient informed and uninformed proposals seem to provide the same overall efficiency in this case but still completely dominate the Kalman alternatives here too.



(a) Average root expected squared jump distance per second for the sequential versions of the auxiliary first order Kalman sampler  $\circ$ , second order Kalman sampler  $\times$ , cSMC sampler  $\square$ , gradient-informed cSMC  $*$  sampler, the guided cSMC  $\bullet$  sampler, and the gradient-informed guided cSMC  $\blacktriangle$  sampler.

(b) Average root expected squared jump distance per second for the parallel versions of the auxiliary first order Kalman sampler  $\circ$ , second order Kalman sampler  $\times$ , cSMC sampler  $\square$ , and gradient-informed cSMC  $*$  sampler. The latter two are hard to distinguish, with no clear difference in terms of performance.

Figure 2: Average (across 10 different experiments) root expected squared jump distance per second for all the sampler considered on the stochastic volatility model.

This underwhelming performance of the Kalman sampler was in fact to be expected given the need to solve 250 matrix systems of dimension 30 per iteration (albeit some are done in parallel on GPU). In fact, this had another deleterious effect: the parallel versions of the auxiliary Kalman sampler suffered from numerical divergence in this experiment when using single precision floats (32-bits representation). This problem, due to the numerical instability of the covariance matrices calculations is well known in the literature (see, e.g. Bierman, 1977) and prompted the development of a square-root version of the parallel Kalman filtering and smoothing algorithms in Yaghoobi et al. (2022). Here, we instead simply used double precision floats instead of the square-root method as this sufficed to fix the numerical instability. This numerical instability is an important drawback of Kalman methods in general, and is particularly salient on parallel hardware which is often optimised to run on lower precision arithmetic (Jouppi et al., 2017). The issue did not arise for the sequential version of the algorithms, and we therefore stuck to single float precision arithmetic for these. In the next section, we show how latent structure can be leveraged to bypass the dimensionality problem.

### 5.3 Spatio-temporal model

Finally, we consider the spatio-temporal model of Crucinio and Johansen (2022, Section 4.2) which was recently introduced as a benchmark for high-dimensional state inference in non-linear systems. It consists in independent latent dynamics for a state  $X_t(i, j)$  located on a two-dimensional lattice  $\{1, \dots, d\} \times \{1, \dots, d\} \ni (i, j)$ , for  $d = 8$ , with an observation model that does not factorise over the nodes of the lattice, thereby creating non-trivial posterior structure between the states. We are given a  $8^2 = 64$  dimensional model

$$\begin{aligned} X_t(i, j) &= X_{t-1}(i, j) + U_t(i, j), \quad i, j = 1, \dots, d, \\ Y_t(i, j) &= X_t(i, j) + V_t(i, j), \quad i, j = 1, \dots, d, \end{aligned} \tag{54}$$

where, for all  $t, i, j$ , the  $U_t(i, j)$  are i.i.d. according to  $\mathcal{N}(0, \sigma_X^2)$ , and for all  $t$ , the  $V_t$ 's are i.i.d. according to a multivariate t-distribution with  $\nu$  degrees of freedom centred on 0. The precision matrix of the  $V_t$ 's

is given by  $\Sigma^{-1} = \tau^{D[(i,j),(i',j)]}$  if  $D[(i,j),(i',j)] \leq r_y$  and 0 otherwise, where  $D[(i,j),(i',j)]$  is a graph distance, and  $\tau < 0$  a given parameter.

In [Crucinio and Johansen \(2022\)](#), the parameters are chosen to be  $\sigma_X = 1$ ,  $\nu = 10$ ,  $\tau = -1/4$ ,  $r_y = 1$ , and  $D[(i,j),(i',j)] = |i - i'| + |j - j'|$ , so that an observation is mostly corrupted by its direct neighbours. We keep all the parameters unchanged, with the exception that, in order to make the problem more difficult, we take  $\nu = 1$  so that the observation model does not have first or second moments, and to showcase the parallelisation in time, we also consider a substantially higher number of time steps  $T = 1024$  (vs.  $T = 10$  in [Crucinio and Johansen, 2022](#)). Overall, the total dimension of the target model is therefore of the order of 65 000. The first order auxiliary Kalman sampler is particularly suited to this type of model, even if the underlying state dimension is large. This is due to the fact that the prior factorises across all dimensions, so that the auxiliary LGSSM proposal (24) factorises too, even if the target  $\pi(x_{0:T})$  does not. As a consequence, we are left with sampling from  $d \times d$  independent one-dimensional LGSSMs rather than a  $d \times d$  dimensional one. This means that, instead of needing to compute conditional Gaussian distributions of dimension  $d \times d$ , and therefore needing to solve systems of size  $d \times d$ , we only need to solve one-dimensional systems, that is, divide by scalars. This property extends to some extent to auxiliary cSMC samplers where the proposal is chosen to factorise across dimensions too. This means that the cost will be dominated by the computation of the log-likelihood of the multivariate t-distribution at each time step and (for specialised implementations) the complexity of the auxiliary cSMC will then be a direct multiple of the complexity of the auxiliary Kalman sampler. This property is not verified in the case of “full” prior dynamics as we will see in [Section 5.2](#).

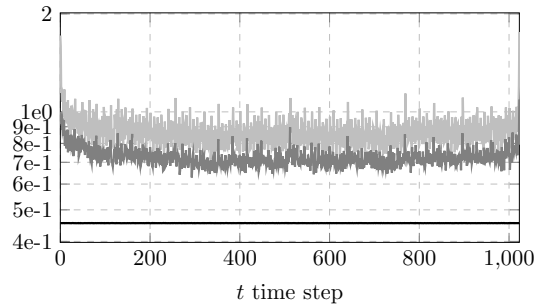
The experiment design is as follows: we simulate 20 datasets from (54). For each of these, we set the initial trajectory of the MCMC chain to be the result of a single trajectory formed from the backward sampling ([Godsill et al., 2004b](#)) of a bootstrap filter algorithm with 1 000 particles (this gives bad smoothing statistics but is a good starting point for a MCMC chain) and run  $A = 5\,000$  adaptation steps, after which the statistics of the chain are collected over  $L = 20\,000$  iterations. For this experiment, all the sequential versions of the auxiliary Kalman and cSMC samplers were dramatically slower than the parallel-in-time alternatives: they took in the order of a second per iteration, both on CPU and GPU, compared to the PIT versions that took in the order of a millisecond per iteration on GPU. As a consequence, we do not report their results here. Instead, we focus on (i) the parallel-in-time version of [Finke and Thierly \(2023\)](#) given by using [Corenfos et al. \(2022\)](#) on step 3 of [Algorithm 3](#), (ii) the parallel-in-time version of the gradient auxiliary proposal (43) of [Section 4.3](#), which we refer to as gradient-informed, and finally (iii) the auxiliary Kalman sampler (14) of [Section 2.2](#), with first order linearisation only, noting that the second order would remove the benefits of having a separable prior.

For the gradient-informed and standard parallel-in-time cSMC samplers we pick  $N = 25$  particles and we target an acceptance rate per time step of 25%. This is more conservative than in [Finke and Thierly \(2023\)](#) as we found that the samplers struggled to calibrate themselves when too high values were picked. As per [Titsias and Papaspiliopoulos \(2018\)](#), we target a 50% acceptance rate for the auxiliary Kalman sampler. The final average acceptance rates were a little lower, with the auxiliary Kalman sampler accepting 34% of the trajectories, and the two versions of the auxiliary cSMC around 23%. This is most likely due to our calibration algorithm being too optimistic, but did not seem to impact the final results beyond reason and therefore did not, in our opinion, warrant further investigation.

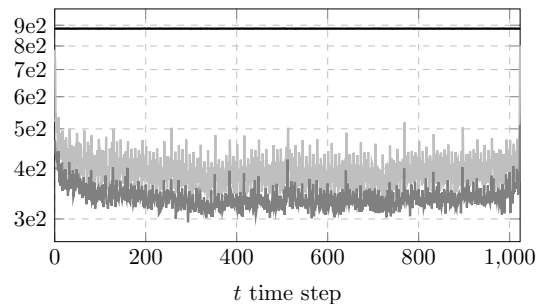
The RESJD is shown, averaged over all experiments, in [Figure 3a](#), while the time scaled RESJD, namely RESJD divided by the number of seconds taken to run one step of the sampler is shown, averaged over all experiments, in [Figure 3b](#).

As can be seen in the figure, the gradient-enhanced PIT auxiliary cSMC has a better RESJD than the basic PIT auxiliary cSMC which in turn has a better RESJD than the auxiliary Kalman sampler. The ordering of these methods however changes if one takes into account the additional complexity incurred by SMC, and after rescaling by the time taken by iteration, the auxiliary Kalman sampler dominates the gradient-enhanced PIT auxiliary cSMC which still dominates its basic counterpart.

In practice, the auxiliary Kalman, conditional SMC, and gradient-enhanced conditional SMC samplers took respectively in average 0.52, 2.1, and 2.2 milliseconds per iteration. While some idiosyncrasies may be present due to the Hastings acceptance step present in [Algorithm 1](#) and not in the cSMC algorithm, we believe that this performance gap could be further improved by a careful consideration of the structure of the model in the Kalman sampler – which we have not undertaken here in order to preserve the general applicability of our implementation.



(a) Root expected squared jump distance for the auxiliary Kalman sampler —, the auxiliary cSMC sampler —, and the auxiliary cSMC sampler with gradient-informed proposals —. Kalman — shows as a roughly horizontal line at the bottom.



(b) Root expected squared jump distance per second for the auxiliary Kalman sampler —, the auxiliary cSMC sampler —, and the auxiliary cSMC sampler with gradient-informed proposals —.

Figure 3: Average (across 20 different experiments) root expected squared jump distance per iteration and second for all the samplers considered on the spatio-temporal model (54).

## 6 Discussion

In this article, we have presented a principled approach to doing MCMC-based inference in general tractable Feynman–Kac models. At core, the method corresponds to augmenting the model by introducing an artificial observation model, and then proceeding to sample from the augmented model using a two step approach: first sample the observations conditionally on a trajectory, and second, sample from a MCMC kernel keeping the trajectory conditional distribution invariant.

To summarise, we have described two versions of this class of samplers. A first one, which we coined auxiliary Kalman sampler can be seen as an extension/specialisation of Titsias and Papaspiliopoulos (2018) to models with latent dynamics, and is particularly useful when the latent model is quasi-Gaussian and of relatively small dimension. The second class, which considers using conditional SMC to sample the trajectory conditional to the auxiliary observations, can be seen as a generalisation of Finke and Thiery (2023). Importantly, we have shown that both methods introduced could be parallelised across time steps on hardware such as GPUs, while retaining good statistical properties: the sequential and parallel versions of the auxiliary Kalman sampler are fully statistically equivalent, while the particle Gibbs ones are not, but the parallel-in-time auxiliary particle Gibbs does not suffer from worse mixing properties, in particular when run time is taken into account.

At least three classes of latent Markovian models elude our auxiliary Kalman samplers:

1. Models with intractable transition or observation density, for which we cannot compute the unnormalised smoothing density.
2. Models with multi-modal posteriors, which are hard for MCMC methods in general due to the “local” perspective they take. This can, however, be handled by combining the method with meta-algorithms, such as parallel tempering (Geyer, 1991).
3. Models with very non-Gaussian latent dynamics or observations, such as those exhibiting multiplicative noise or presenting boundary constraints akin to discontinuities.

Another, softer, issue is concerned with the computational complexity of the method with respect to the dimension of the latent space  $d_X$ . Indeed, because Kalman filtering and backward sampling relies on recursive Gaussian conditioning, it requires to compute matrices inverses of size  $d_X \times d_X$  (or more precisely, to solve systems of the same size). In models where no specific structure alleviates these computations, they can quickly become computationally overwhelming as the dimension of the latent space increases.

Replacing the LGSSM proposal of Section 2.2 by a local conditional SMC update as per Section 4 allowed us to trade the single expensive computation for a quick computation across several particles. This also partially alleviates the other issues with Kalman approximations. However, the usual issues with cSMC remain: several trajectories need to be simulated, and the fully adapted auxiliary cSMCs of Section 4.3 cannot be parallelised-in-time. They however do not solve the problem of intractable densities, or multimodality.

While the complexity issue is somewhat mitigated by the auxiliary particle Gibbs samplers, it still remains to some extent, in particular when using dynamics-adapted proposals, which require computing a Kalman gain matrix, thereby involving an inversion of a  $d_x \times d_x$  matrix. A possibility, not explored in this article, is to consider other families of proposal distributions than LGSSMs – either in the auxiliary Kalman or the auxiliary particle Gibbs case. In particular, ensemble Kalman (Frei and Künsch, 2013) approximations can be used as a natural proposal substitute to breach the computational barrier while still retaining asymptotic Monte Carlo exactness. It is likely that such proposals would perform particularly well when they form reasonable local approximations in the first place.

The reformulation of Finke and Thiery (2023) as a conditional SMC within a Gibbs sampler is a particularly promising avenue as it invites the direct application of the many cSMC practical and theoretical technologies developed over the past decade. Our experiments showed that leveraging this representation to design better auxiliary proposal distributions already largely improved the statistical properties of the algorithm at a very low additional computational cost. Interestingly, the main benefit came from introducing gradients in the proposal, rather than incorporating the dynamics themselves. This is likely because the potentials have been designed to be particularly informative compared to the dynamics (in order to increase the variance of the underlying particle filter). We believe that this can still be improved upon many-fold in a number of settings. A natural first step would be to combine these with methods developed to tackle degeneracy in particle Gibbs (e.g. Lindsten et al., 2015) or very long time series (Karppinen et al., 2022).

A classical way to improve mixing in particle Gibbs is by means of blocking (see, e.g. Singh et al., 2017). This is typically done in the time dimension, where the Markovian structure is leveraged to sample independent blocks  $(t_1, t_2)$ ,  $(t_3, t_4)$ ,  $\dots$ , conditionally on their extremities. In the case of our auxiliary Kalman samplers, another type of blocking is possible, and consists in implementing a coordinate-wise blocking which is akin to introducing an additional level in the proposed Hastings-within-Gibbs sampler. This is possible due to the fact that, for a coordinate  $d$ , the posterior distribution of the coordinate path conditionally on the rest of the coordinates is still of the form (4).

A final remark is concerned with the implementation of the prefix-sum algorithm Blelloch (1989) in the JAX library (Bradbury et al., 2018). At the time of writing this article, the JAX implementation can be considered high-level, by which we mean that the algorithm is implemented in Python (Van Rossum and Drake, 2009) rather than natively using the CUDA (NVIDIA et al., 2022) GPU backend. This is in contrast to other control flow primitives such as loops and "if-else" branching. We do expect that a native implementation of the algorithm, fully GPU-focused would improve the time-performance of the Kalman samplers.

## Individual Contributions

The original idea, methodology, implementation, and redaction of the first version of this article are due to Adrien Corenflos. Simo Särkkä contributed the method of Section 3.2 and reviewed the final version of the manuscript.

## Acknowledgments

The first author would like to warmly thank Nicolas Chopin for pointing out the link between the first method presented in this article and Titsias and Papaspiliopoulos (2018). Some of the cSMC ideas presented in this article also stemmed from discussions and presentations that took place at the "Computational methods for unifying multiple statistical analyses" (Fusion) workshop organised by Rémi Bardenet, Kerrie Mengersen, Pierre Pudlo, and Christian Robert in Centre International de Rencontres Mathématiques (CIRM) in October 2022. Both authors gratefully acknowledge funding from the Academy of Finland, project 321891 (ADAFUME), and project 321900 (PARADIST).

## References

- Andrieu, C., Doucet, A., and Holenstein, R. (2010). Particle Markov chain Monte Carlo methods. *Journal of the Royal Statistical Society: Series B (Statistical Methodology)*, 72(3):269–342.
- Andrieu, C., Lee, A., and Vihola, M. (2018). Uniform ergodicity of the iterated conditional SMC and geometric ergodicity of particle Gibbs samplers. *Bernoulli*, 24(2):842–872.

- Andrieu, C. and Roberts, G. O. (2009). The pseudo-marginal approach for efficient Monte Carlo computations. *The Annals of Statistics*, 37(2):697 – 725.
- Barfoot, T. D. (2017). *State estimation for robotics*. Cambridge University Press.
- Bell, B. M. (1994). The iterated Kalman smoother as a Gauss–Newton method. *SIAM Journal on Optimization*, 4(3):626–636.
- Bezanson, J., Edelman, A., Karpinski, S., and Shah, V. B. (2017). Julia: A fresh approach to numerical computing. *SIAM Review*, 59(1):65–98.
- Bierman, G. J. (1977). *Factorization Methods for Discrete Sequential Estimation*. Academic Press.
- Blelloch, G. E. (1989). Scans as primitive parallel operations. *IEEE Transactions on Computers*, 38(11):1526–1538.
- Bradbury, J., Frostig, R., Hawkins, P., Johnson, M. J., Leary, C., Maclaurin, D., and Wanderman-Milne, S. (2018). JAX: composable transformations of Python+NumPy programs. <http://github.com/google/jax>.
- Chopin, N. and Papaspiliopoulos, O. (2020). *An Introduction to Sequential Monte Carlo*. Springer.
- Chopin, N. and Singh, S. S. (2015). On particle Gibbs sampling. *Bernoulli*, 21(3):1855–1883.
- Corenflos, A., Chopin, N., and Särkkä, S. (2022). De-sequentialized Monte Carlo: a parallel-in-time particle smoother. *Journal of Machine Learning Research*, 23(283):1–39.
- Crucinio, F. R. and Johansen, A. M. (2022). A divide and conquer sequential Monte Carlo approach to high dimensional filtering. *arXiv preprint arXiv:2211.14201*.
- Dau, H.-D. and Chopin, N. (2022). On the complexity of backward smoothing algorithms. *arXiv preprint arXiv:2207.00976*.
- de Jong, P. and Shephard, N. (1995). The simulation smoother for time series models. *Biometrika*, 82(2):339–350.
- Del Moral, P. (2004). *Feynman-Kac Formulae: Genealogical and Interacting Particle Systems with Applications*. Springer New York, New York, NY.
- Deligiannidis, G., Doucet, A., and Pitt, M. K. (2018). The correlated pseudomarginal method. *Journal of the Royal Statistical Society: Series B (Statistical Methodology)*, 80(5):839–870.
- Douc, R., Garivier, A., Moulines, E., and Olsson, J. (2011). Sequential Monte Carlo smoothing for general state space hidden Markov models. *The Annals of Applied Probability*, 21(6):2109–2145.
- Doucet, A. (2010). A note on efficient conditional simulation of Gaussian distributions. Technical report, University of British Columbia.
- Finke, A. and Thiery, A. H. (to appear, 2023). Conditional sequential Monte Carlo in high dimensions. *Annals of Statistics*.
- Frei, M. and Künsch, H. R. (2013). Bridging the ensemble Kalman and particle filters. *Biometrika*, 100(4):781–800.
- Frühwirth-Schnatter, S. (1994). Data augmentation and dynamic linear models. *Journal of Time Series Analysis*, 15(2):183–202.
- García-Fernández, Á. F., Svensson, L., and Särkkä, S. (2017). Iterated posterior linearization smoother. *IEEE Transactions on Automatic Control*, 62(4):2056–2063.
- Geman, S. and Geman, D. (1984). Stochastic relaxation, Gibbs distributions, and the Bayesian restoration of images. *IEEE Transactions on pattern analysis and machine intelligence*, PAMI-6(6):721–741.
- Geyer, C. J. (1991). Markov chain Monte Carlo maximum likelihood. *Interface Proceedings*.
- Godsill, S. J., Doucet, A., and West, M. (2004a). Monte Carlo smoothing for nonlinear time series. *Journal of the American Statistical Association*, 99(465):156–168.

- Godsill, S. J., Doucet, A., and West, M. (2004b). Monte Carlo smoothing for nonlinear time series. *Journal of the American Statistical Association*, 99(465):156–168.
- Guarniero, P., Johansen, A. M., and Lee, A. (2017). The iterated auxiliary particle filter. *Journal of the American Statistical Association*, 112(520):1636–1647.
- Hastings, W. K. (1970). Monte Carlo sampling methods using Markov chains and their applications. *Biometrika*, 57(1):97–109.
- Jazwinski, A. H. (1970). *Stochastic Processes and Filtering Theory*. Academic Press.
- Jouppi, N. P., Young, C., Patil, N., Patterson, D., Agrawal, G., Bajwa, R., Bates, S., Bhatia, S., Boden, N., Borchers, A., et al. (2017). In-datacenter performance analysis of a tensor processing unit. In *Proceedings of the 44th annual international Symposium on Computer Architecture*, pages 1–12.
- Julier, S. J. and Uhlmann, J. K. (2004). Unscented filtering and nonlinear estimation. *Proceedings of the IEEE*, 92(3):401–422.
- Karppinen, S., Singh, S. S., and Vihola, M. (2022). Conditional particle filters with bridge backward sampling. *arXiv preprint arXiv:2205.13898*.
- Kitagawa, G. (1996). Monte Carlo filter and smoother for non-Gaussian nonlinear state space models. *Journal of Computational and Graphical Statistics*, 5(1):1–25.
- Klaas, M., Freitas, N. d., and Doucet, A. (2005). Toward practical  $N^2$  Monte Carlo: the marginal particle filter. In *Proceedings of the Twenty-First Conference on Uncertainty in Artificial Intelligence*, pages 308–315.
- Lee, A., Singh, S. S., and Vihola, M. (2020). Coupled conditional backward sampling particle filter. *The Annals of Statistics*, 48(5):3066–3089.
- Leisen, F. and Mira, A. (2008). An extension of Peskun and Tierney orderings to continuous time Markov chains. *Statistica Sinica*, pages 1641–1651.
- Lindsten, F., Bunch, P., Singh, S. S., and Schon, T. B. (2015). Particle ancestor sampling for near-degenerate or intractable state transition models. *arXiv preprint arXiv:1505.06356*.
- Lindsten, F., Jordan, M. I., and Schön, T. B. (2014). Particle Gibbs with ancestor sampling. *Journal of Machine Learning Research*, 15:2145–2184.
- Lindsten, F., Schön, T., and Jordan, M. (2012). Ancestor sampling for particle Gibbs. *Advances in Neural Information Processing Systems*, 25.
- Malory, S. J. (2021). *Bayesian Inference for Stochastic Processes*. Lancaster University (United Kingdom).
- Metropolis, N., Rosenbluth, A. W., Rosenbluth, M. N., Teller, A. H., and Teller, E. (1953). Equation of state calculations by fast computing machines. *The Journal of Chemical Physics*, 21(6):1087–1092.
- Mider, M., Schauer, M., and Van der Meulen, F. (2021). Continuous-discrete smoothing of diffusions. *Electronic Journal of Statistics*, 15(2):4295–4342.
- Müller, P. (1993). Alternatives to the Gibbs sampling scheme. Technical report, Institute of Statistics and Decision Sciences, Duke Univ.
- Murphy, K. and Russell, S. (2001). *Rao-Blackwellised Particle Filtering for Dynamic Bayesian Networks*, pages 499–515. Springer New York, New York, NY.
- Neal, R. M. (2003). Markov chain sampling for non-linear state space models using embedded hidden Markov models.
- NVIDIA, Vingelmann, P., and Fitzek, F. H. (2022). CUDA, release: 11.8.x.
- Pasarica, C. and Gelman, A. (2010). Adaptively scaling the Metropolis algorithm using expected squared jumped distance. *Statistica Sinica*, pages 343–364.
- Peskun, P. H. (1973). Optimum Monte-Carlo sampling using Markov chains. *Biometrika*, 60(3):607–612.

- Särkkä, S. (2013). *Bayesian filtering and smoothing*. Cambridge University Press.
- Särkkä, S. and García-Fernández, Á. F. (2021). Temporal parallelization of Bayesian smoothers. *IEEE Transactions on Automatic Control*, 66(1):299–306.
- Singh, S. S., Lindsten, F., and Moulines, E. (2017). Blocking strategies and stability of particle Gibbs samplers. *Biometrika*, 104(4):953–969.
- Tierney, L. (1998). A note on Metropolis-Hastings kernels for general state spaces. *Annals of applied probability*, pages 1–9.
- Titsias, M. K. and Papaspiliopoulos, O. (2018). Auxiliary gradient-based sampling algorithms. *Journal of the Royal Statistical Society: Series B (Statistical Methodology)*, 80(4):749–767.
- Tjelmeland, H. (2004). Using all Metropolis–Hastings proposals to estimate mean values. Technical report, NTNU.
- Tronarp, F. (2020). *Iterative and Geometric Methods for State Estimation in Non-linear Models*. PhD thesis, Aalto University.
- Tronarp, F., García-Fernández, Á. F., and Särkkä, S. (2018). Iterative filtering and smoothing in nonlinear and non-Gaussian systems using conditional moments. *IEEE Signal Processing Letters*, 25(3):408–412.
- Van Rossum, G. and Drake, F. L. (2009). *Python 3 Reference Manual*. CreateSpace, Scotts Valley, CA.
- Wan, E. A. and Van Der Merwe, R. (2000). The unscented Kalman filter for nonlinear estimation. In *Proceedings of the IEEE 2000 Adaptive Systems for Signal Processing, Communications, and Control Symposium*, pages 153–158. IEEE.
- Whiteley, N. (2010). Discussion on particle Markov chain Monte Carlo methods. *Journal of the Royal Statistical Society: Series B*, 72(3):306–307.
- Yaghoobi, F., Corenflos, A., Hassan, S., and Särkkä, S. (2021). Parallel iterated extended and sigma-point Kalman smoothers. In *ICASSP 2021-2021 IEEE International Conference on Acoustics, Speech and Signal Processing (ICASSP)*, pages 5350–5354. IEEE.
- Yaghoobi, F., Corenflos, A., Hassan, S., and Särkkä, S. (2022). Parallel square-root statistical linear regression for inference in nonlinear state-space models. *arXiv preprint arXiv:2207.00426*.